PHYSICS OF EXTREMELY HIGH ENERGY COSMIC RAYS

XAVIER BERTOU, MURAT BORATAV, ANTOINE LETESSIER-SELVON

Laboratoire de Physique Nucléaire et des Hautes Energies (IN2P3/CNRS), Universités Paris 6&7, 4 place Jussieu 75005 Paris, France

Over the last third of the century, a few tens of events, detected by ground-based cosmic ray detectors, have opened a new window in the field of high-energy astrophysics. These events have macroscopic energies - exceeding 5×10^{19} eV -, unobserved sources - if supposed to be in our vicinity -, an unknown chemical composition and a production and transport mechanism yet to be explained. With a flux as low as one particle per century per square kilometer, only dedicated detectors with huge apertures can bring in the high-quality and statistically significant data needed to answer those questions. In this article, we review the present status of the field both from an experimental and theoretical point of view. Special attention is given to the next generation of detectors devoted to the thorough exploration of the highest energy ranges.

1. Introduction

This review article will mainly concern the problems raised by the existence and observation of cosmic rays whose energies are above 5×10^{19} eV. Such cosmic rays - for which we shall use the term "extremely high energy cosmic rays" or EHECR - are exceptional for the following reasons:

- The Greisen-Zatsepin-Kuzmin (GZK) cutoff[1] corresponds to the threshold for inelastic collisions between the cosmic microwave background (CMB) and protons (photo-pion production) or heavy nuclei (photo-disintegration). Similar cutoffs exist at lower energies for gammas interacting with background photons (CMB, infra-red or radio waves). Consequently, and except for neutrinos, if the EHECR observed on Earth are due to the known stable particles, they must be produced in our vicinity. At the GZK cutoff, the "visible" universe shrinks suddenly to a sphere of a few tens of megaparsecs (Mpc).[a] This should be reflected on the energy spectrum of cosmic rays as a sharp drop around 5×10^{19} eV. The available data show no such drop. On the contrary, if a structure exists in the energy spectrum, it is in the sense of a softening of the power law, possibly suggesting a new component rising from under an otherwise steeply falling spectrum.
- There are very few conventional astrophysical sources considered by the experts as being able to accelerate particles at energies exceeding those of the

[a] The megaparsec is the cosmological unit of distance that we shall use throughout this article. $1\,\mathrm{Mpc} = 3.26 \times 10^{6}$ light-years $\approx 3 \times 10^{19}$ km

most energetic EHECR that have been observed in the past.

- At such energies, the bending effect of the galactic and extragalactic magnetic fields are quite weak on the EHECR. Thus, even if they are charged particles, their reconstructed incident direction should point toward their sources within a few degrees. This distinguishes the EHECR from their counterparts in the lower energy regions: one can use them for point-source-search astronomy.

The widely shared excitement about the EHECR comes from the above considerations and from the study of the scarce data available. The EHECR exist. They have to be produced somewhere and with a mechanism we do not understand up to now: to explain the observation of the highest energy events, the energy at the source should probably be in the ZeV range (Z is for *zetta*, i.e. 10^{21}), namely at least 150 joules! If these extraordinary accelerating engines are astrophysical macroscopic objects, they must be visible through some counterpart that e.g. optical- or radio-astronomy should detect. But no such remarkable object is visible in the directions from where the EHECR come. There is even no convincing evidence that one can find any correlation between the incoming directions and the inhomogeneous distribution of matter in our vicinity.

During the 35 years where the EHECR puzzle was fed by a slow input of experimental data, many models and theories were put forward to try to explain it. In the following, we shall develop in detail the facts and arguments briefly mentioned in this introduction. In section 2 we discuss the cosmic ray interactions in the atmosphere and the detection techniques. In section 3 we review our current knowledge of the subject while section 4 is devoted to transport problems and to candidate source characteristics. Finally section 5 describes the next generation of detectors devoted to EHECR studies.

There is no doubt that for the scientists working in the field of what is now called "Particle Astrophysics" the near future will be a thrilling period where a large variety of models or theories will be confronted with high-quality and high-statistical data brought by a new generation of detectors.

To avoid repetitive use of large powers of ten, the energy units in the following will mostly be in zetta-electron-volts (ZeV, see above) and exa-electron-volts (EeV, i.e. 10^{18} eV).

2. The detection of the EHECR

When the cosmic ray flux becomes smaller than 1 particle per m^2 per year, satellite borne detectors are not appropriate any more. This happens above 10^{16} eV (the so-called "knee" region). Then large surfaces are needed. The detectors then become ground-based. What they detect is not the incident particle itself but the cascade of secondary particles initiated by the cosmic ray interactions with the molecules of the atmosphere. The object of study is therefore this cascade or shower called the *Extensive Air Shower* (EAS).

Another distinction has to be made between the techniques used at lower and higher energies. Air showers can actually be observed at much lower energies than the knee region. Gamma ray astronomy, for example, uses the properties of the EAS (production of Cerenkov light by charged secondaries in the atmosphere) to detect and measure cosmic photons from a few tens of GeV up. The main difference with the higher energies is that above a few hundreds of TeV and up to 10^{20} eV, cosmic rays are mainly charged particles which cannot be associated with a point source as is the case with photons. Therefore a ground-based cosmic ray detector must survey the whole sky and not point at a defined source.

There are two major techniques used in the detection of the highest energy cosmic rays. The first, and the most frequent, is to build an array of sensors (scintillators, water Cerenkov tanks, muon detectors) spread over a large area. The detectors count the particle densities at any given moment, thus sampling the EAS particles hitting the ground. The surface of the array is chosen in adequation with the incident flux and the energy range one wants to explore (large array surfaces for weak fluxes, large density of sensors for lower energies). From this sampling of the lateral development of the shower at a given atmospheric depth one can deduce the direction, the energy and possibly the identity of the primary CR. The second technique, until recently the exclusivity of a group from the University of Utah, consists in studying the longitudinal development of the EAS by detecting the fluorescence light produced by the interactions of the the charged secondaries.

2.1. *The Extensive Air Showers*

On an incident cosmic ray the atmosphere acts as a calorimeter with variable density, a vertical thickness of 26 radiation lengths and about 11 interaction lengths. In the following, we will describe the properties of a vertical EAS initiated by a 10 EeV proton and mention how some of these properties are modified with energy and with the nature of the initial cosmic ray (CR).

At sea level (atmospheric thickness of 1033 g/cm^2) the number of secondaries reaching ground level (with energies in excess of 200 keV) is about 3×10^{10} particles. 99% of these are photons and electrons/positrons in a ratio of 6 to 1. Their energy is mostly in the range 1 to 10 MeV and they transport 85% of the total energy. The remaining 1% is shared between mostly muons with an average energy of 1 GeV (and carrying about 10% of the total energy), pions of a few GeV (about 4% of the total energy) and, in smaller proportions, neutrinos and baryons. The lateral development of the shower is represented by its Molière radius (or the distance within which 90% of the total energy of the shower is contained) which, in the standard air is 70 m. However, the actual extension of the shower at ground level is of course much larger. As an example, at a distance of 1 km from the shower axis, the average densities of photons/electrons/muons are 30/2/1 per m^2.

The longitudinal development of the EAS will be described to some extent in the next section. Let us just mention that the maximum size of the shower is reached at an atmospheric depth of 830 g/cm^2 (or an altitude of about 1800 meters) and contains about 7×10^9 electrons (which produce the fluorescence light detected with the Fly's Eye telescopes, see below).

Showers initiated by heavier nuclei can be described by making use of a superposition principle: a heavy nucleus of mass number A and energy E can be in a first approximation considered as a superposition of A showers initiated by nucleons each with an energy of E/A, therefore less penetrating than a nucleon with energy E (roughly 100 g/cm^2 higher in the atmosphere for iron).

A ground array makes use of two main effects to separate heavy from light nuclei (and from photons): the proportion of muons compared to the electromagnetic component of the shower and the rise time of the detected signal. Both parameters are due to the way the muons are produced during the shower development. The muons in a shower come from the decay of charged pions when they reach an energy low enough so that their decay length becomes smaller than their interaction length. Since this happens earlier in the case of a primary heavy nucleus, the resulting shower is richer in muons than a proton shower. At the same time, and since muons are produced earlier in the shower development, they reach the ground also earlier, compared to the electromagnetic component which undergoes many interactions before reaching the detector array.

For a photon shower the proportion of muons will be even smaller and at the highest energies and another physical process will have important consequences on the EAS detection and characterization. This is the Landau-Pomeranchuk-Migdal (LPM) effect[2] which describes the decrease of the photon/electron nucleus cross-sections with energy and with the density of the medium with which they interact. Even in the upper atmosphere, the LPM effect becomes appreciable at energies in the EeV range so that it is possible for a photon of 100 EeV to develop an EAS very deep in the atmosphere, yielding less than 10^9 particles at ground level. Such a shower would have an extension of only a few km^2.

These effects are studied through heavy use of EAS Monte Carlo programs such as AIRES,[3] CORSIKA,[4] HEMAS[5] or MOCCA.[6] At the EHECR ranges, where the center-of-mass energies are much higher (almost two orders of magnitude) than those attainable in the future (and the most powerful) accelerator LHC, the correct modelling of the EAS in these programs becomes delicate. Some data are available from accelerator experiments such as HERA,[7] and showers of about 10^{16} eV are now being well studied through experiments such as KASCADE.[8] The models are thus constrained at lower energies and then extrapolated at higher ranges.

The most commonly used models for the high energy hadronic interactions of the simulation programs are SIBYLL,[9] VENUS,[10] QGSJet[11] and DPMJet.[12] Interactions at lower energies are either processed through internal routines of the EAS simulation programs or by well-known packages such as GHEISHA.[13] Some detailed studies of the different models are available.[14] A clear conclusion is that the simulation results are never identical, even when the same theoretical models are used in different programs. However, when simulating a shower, these models are only used for the first few interactions and an EAS yields about 10^{10} or 10^{11}

particles at ground level. Therefore the main shower parameters, such as the reconstructed direction and energy of the primary CR, are never strongly dependent on the chosen model. However, the identification of the primary is more problematic. Whatever technique is chosen (see Section 3.4 for details) the parameters used to identify the primary cosmic ray undergo large physical fluctuations which make an unambiguous identification difficult.

A complete analysis done by the KASCADE group on the hadronic core of EAS[8] has put some constraints on interaction models beyond accelerator energies. Various studies seem to indicate QGSJet as being the model which best reproduces the data[14,15] with still some disagreement at the *knee* energies (10^{16} eV). For the highest energies, additionnal work (and data) is needed to improve the agreement between the available models.

2.2. *The optical fluorescence technique*

The idea that one could use the fluorescence light produced in the atmosphere to detect and characterize the EAS was first suggested independently by Greisen and Suga[16] and then by a few other authors in the early sixties. The basic principle is simple[17] (although the detector itself and the measuring techniques are quite sophisticated): the charged particles produced in the development of the EAS excite the nitrogen atoms of the atmosphere which then emit, very quickly and isotropically, fluorescence light which can be detected by a photo-multiplier. The emission efficiency (ratio of the energy emitted as fluorescence light to the deposited one) is poor (less than 1%), therefore observations can only be done on clear moonless nights (which results in an average 10% duty cycle) and low energy showers can hardly be observed. At higher energies, the huge number of particles in the shower[b] produce enough light to be detected even at large distances. The fluorescence yield is 4 photons per electron per meter at ground level. The emitted light is typically in the 300-400 nm UV range to which the atmosphere is quite transparent. Under favorable atmospheric conditions an EHECR shower can be detected at distances as large as 20 km (about two attenuation lengths in a standard desert atmosphere at ground level).

The first successful detectors based on these ideas were built by a group of the University of Utah, under the name of "Fly's Eyes", and used with the Volcano Ranch ground array (see Section 3.2). A complete detector was then installed at Dugway (Utah) and started to take data in 1982. An updated version, the High-Resolution Fly's Eye, or HiRes, is presently running on this same site.

Figure 1 shows the geometry of the detection of an air shower by Fly's Eye type detectors (which are usually given the more generic name of "fluorescence detectors" or "fluorescence telescopes"). The detector sees the shower as a variable light bulb[c] moving at the speed of light along the shower axis. The detector itself is

[b]The highest energy shower ever detected (320 EeV) was observed by the Fly's Eye detector: at the shower maximum, the number of particles was larger than 2×10^{11}.
[c]A rough estimate of the equivalent radiated power would be $3E_{18}$ watts at the shower maximum,

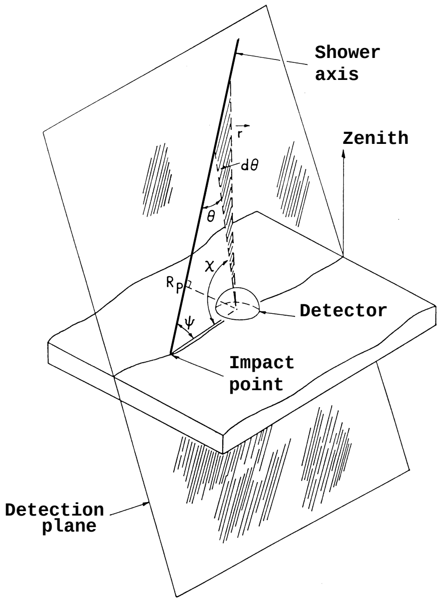

Fig. 1. The principle of the detection of an EAS by a fluorescence telescope.[17]

a set of phototubes mounted on a "camera" set at the focal plane of a mirror. Each phototube sees a small portion of the sky (typically 1°). A fit on the pattern of tubes hit by the fluorescence photons determines with a precision better than one degree the plane containing the detector and the shower axis. In the *stereo mode* (EAS seen by two telescopes installed a few km apart), two planes are thus reconstructed and their intersection gives the incident direction with good precision. In the *mono mode* (EAS seen by a single telescope), one has to rely on the the time of arrival of the photons on the tubes. A good reconstruction of the direction (the Ψ angle) then needs a large number of pixels to be hit, enough to measure simultaneously the angular velocity and the angular acceleration of the shower development. Finally, in the *hybrid mode*, i.e. simultaneous detection of the EAS with a fluorescence telescope *and* a ground array, the knowledge of the intersection of the shower axis with the array plane (reconstructed by the array) allows the selection of the right direction in the family of lines in the detector-shower axis plane. For 100 EeV showers, a precision of 0.2° can then be reached.

The fluorescence technique is the most appropriate way to measure the energy of the incident cosmic ray: it is a partial calorimetric measurement with continuous longitudinal sampling. The amount of fluorescence light emitted is proportional to the number of charged particles in the shower. The EAS has a longitudinal development usually parametrized by the analytic Gaisser-Hillas function giving the size N_e of the shower (actually the number of the ionizing electrons) as a function

where E_{18} is the primary energy in EeV.

of atmospheric depth x:

$$N_e(x) = N_{\max}\left(\frac{x - x_0}{X_{\max} - x_0}\right)^{(X_{\max}-x_0)/\lambda} e^{(X_{\max}-x)/\lambda}$$

where $\lambda = 70\,\mathrm{g/cm}^2$, x_0 is the depth at which the first interaction occurs, and $X_{\max}$ the position of the shower maximum. The total energy of the shower is proportional to the integral of this function, knowing that the average energy loss per particle is 2.2 MeV/g cm^{-2}.

In practice several effects have to be taken into account to properly convert the detected fluorescence signal into the primary CR energy. These include the subtraction of the direct or diffused Cerenkov light, the (wavelength dependent) Rayleigh and Mie (aerosol) scatterings, the dependence of the attenuation on altitude (and elevation for a given altitude) and atmospheric conditions, the energy transported by the neutral particles (neutrinos), the hadrons interacting with nuclei (whose energy is not converted into fluorescence) and penetrating muons whose energy is mostly dumped into the earth. One also has to take into account that a shower is never seen in its totality by a fluorescence telescope: the Gaisser-Hillas function parameters are measured by a fit to the visible part of the shower, usually cut at the beginning (interaction point) and the end (tail absorbed by the earth). All these effects contribute to the systematic errors in the energy measurement which needs sophisticated monitoring and calibration techniques, e.g the use of powerful laser beams shot through the atmosphere. The overall energy resolution one can reach with a fluorescence telescope is of course dependent on the EAS energy but also on the detection mode (mono, stereo or hybrid). The HiRes detector should have a resolution of 25% or better above 30 EeV in the *mono* mode. This improves significantly in the stereo or hybrid modes (about 3% *median* relative error at the same energy in the latter case).

The identification of the primary cosmic ray with a fluorescence telescope is based on the shower maximum in the atmosphere ($X_{\max}$) which depends on the nature and the energy of the incident cosmic ray. At a given energy, and on the average, a shower generated by a heavy nucleus reaches its maximum higher in the atmosphere than that of a light nucleus or a proton. Simulations show typical values of (respectively for iron nuclei and protons) 750 and 850 g/cm^2. Unfortunately, physical fluctuations of the interaction point and of the shower development (larger than the precision on the shower reconstruction) blur this ideal image. As an example, at 10 EeV the typical fluctuation on the $X_{\max}$ position is 50 g/cm^2. Thus, when the fluorescence technique is used alone, it is practically impossible to define the primary composition on a shower-by-shower basis. Therefore, one must look for statistical means of studying the chemical composition and/or use the hybrid detection method where a multi-variable analysis becomes possible.

The former method uses the so-called *elongation rate* measured for a sample of showers within some energy range. The depth of the shower maximum as a function of the energy for a given composition is given by[19]:

$$X_{\max} = D_{\rm el} \ln \left(\frac{E}{E_0} \right)$$

where E_0 is a parameter depending on the primary nucleus mass. Therefore, incident samples of pure composition will be displayed as parallel straight lines with the same slope $D_{\rm el}$ (the *elongation rate*) on a semi-logarithmic diagram. The results of such an analysis in the highest energy range will be mentioned in Section 3.

2.3. *The ground array technique*

A ground array is a set of particle detectors distributed as a more or less regular matrix over some surface. The surface of the array is a direct function of the expected incident flux and of the statistics needed to answer the questions at hand. The 100 km^2 AGASA array (see Section 3.2) is appropriate to confirm the existence of the EHECR with energies in excess of 100 EeV (which it detects at a rate of about one event per year). To explore the properties of these cosmic rays and hopefully answer the open question of their origin, the relevant detector will no doubt be the Auger Observatory with its 6000 km^2 surface over two sites.

The array detectors count the number of secondary particles which cross them as a function of time. Therefore, they sample the non-absorbed part of the shower which reaches the ground. The incident CR's direction and energy are measured by assuming that the shower has an axial symmetry. This assumption is valid for not too large zenith angles (usually $\theta < 60°$). At larger angles the low energy secondaries are deflected by the geomagnetic fields and the analysis becomes more delicate.

The direction of the shower axis (hence of the incident CR) is reconstructed by fitting an analytical function (the "lateral distribution function" or LDF) to the measured densities. The LDF explicit form depends on each experiment. The Haverah Park experiment[20] (an array of water-Cerenkov tanks) used the function:

$$\rho(r, \theta, E) = k r^{-[\eta(\theta,E)+r/4000]}$$

as the LDF for distances less than 1 km from the shower core. Here r is in meters, and η can be expressed as:

$$\eta(\theta, E) = a + b \sec\theta + c \log(E/E_0)$$

with appropriate values for all the parameters taken from shower theory and Monte Carlo studies at a given energy range. At larger distances (and highest energies), this function has to be modified to take into account a change in the rate at which the densities decrease with distance. A much more complicated form is used by the AGASA group.[21] However, the principle remains the same.

Once the zenith angle correction is made for the LDF, an estimator of the primary CR energy is extracted from this function. At energies below 10 EeV, this estimator is usually taken as the particle density (whatever particles detected by the array stations) at 600 m from the shower core, ρ_{600}. The density at 600 m is chosen for the following reason. Because of variations on the primary interaction point (and the position of the shower maximum), there are large fluctuations in the ground densities close to the core. At the same time, the statistical fluctuations in the measured densities are important at large distances where the densities are low. Monte Carlo studies show that somewhere in between, the overall fluctuation reaches a minimum. This happens to be at 600 m from the core, a value slowly increasing when one goes to the highest energies. In the EHECR range, a more appropriate density is ρ_{1000}. Once this value is determined, the primary energy is related to it by a quasi-linear relation:

$$E = k\rho_{600}^{\alpha}$$

where α is a parameter close to 1. Of course, to be able to reconstruct the LDF, many array stations have to be hit at the same time by a shower. The spacing between the stations determines the threshold energy for a vertical shower: the 500 m spacing of the Haverah Park triggering stations corresponds to a threshold of a few 10^{16} eV, while the 1.5 km separation of the Auger Observatory stations makes this array almost 100% efficient for energies above 10 EeV.

In a ground array, the primary cosmic ray's identity is reflected in the proportion of muons among the secondaries at ground level. Here a proper estimator is therefore the ratio of muons to electrons - and eventually photons, if they are detected - (see Section 2.1). When a ground array has muon detecting capabilities (water Cerenkov tanks, buried muon detectors), one measures directly the muon to electron ratio. Otherwise, an indirect method consists in measuring the rise-time of the signal in the detectors: the faster this time, the higher the muon content.

2.4. *The detection of neutrinos*

EHE neutrinos may also be detected by their EAS. This is important for two reasons. The first is that the detection of neutrinos (together with an important component of photons) in the higher energy range of the spectrum is a solid signature of the top-down mechanisms (see Section 4.3). The second is that the projected high energy neutrino telescopes (under-water or under-ice km scale detectors) are ineffective at energies above 10^{16} eV at which the Earth becomes opaque to upward going neutrinos. Therefore large ground arrays (or fluorescence telescopes) for which the interaction medium is not the earth but the atmosphere, and which *could* become efficient enough at 10^{17} eV and above, would be complementary to the neutrino telescopes in the exploration of the whole spectrum.

The neutrino cross-sections at these ultra-high energies become non-negligible (about 10^{-32} cm^2 at 1 EeV).[22] The neutrino can therefore initiate a shower at some point in the atmosphere where the density is high enough. The main difficulty for an observer is to identify the EAS as coming from a neutrino. With the fluorescence technique (which can locate with some precision the interaction point), a clear neutrino signature would be to see a shower starting deep in the atmosphere. However, the expected low fluxes of neutrinos combined with the low cross-sections result in very low event rates. The 10% duty cycle of the fluorescence detectors will therefore hinder their use for this purpose.

An alternative and promising way of detecting ultra-high energy neutrinos would be to use horizontal air showers,[23] i.e. showers generated by cosmic rays with incident zenith angles larger than 60°. At these large angles, hadronic showers have their electromagnetic part extinguished as they have gone through a few equivalent vertical atmosphere (2 at 60°, 3 at 70°, 6 at 80°). Only high energy muons survive past 2 equivalent vertical atmospheres. These muons are created in the first stages of the shower development, are of very high energy, and therefore the shape of the shower front is quite specific: it is very flat (curvature of more than 100 km), and its time extension is very short (less than 50 ns!). On the other hand, a neutrino shower which would have been initiated a few kilometers before hitting the array would appear as a "normal" shower, with a curved front (curvature of a few km), a large electromagnetic component, and a signal with a width of a few microseconds.

With such important differences between neutrino and background (hadronic) showers, particularly at large zenith angles, we can assume that if the fluxes are high enough, the next generation of experiments will detect neutrino induced showers. The real background would come, but only at the highest energies, from penetrating photon showers whose development is delayed due to the LPM effect. However, such showers would show a strong correlation in direction with the geomagnetic field, a helpful effect to distinguish them from neutrinos. A large amount of ongoing work is exploring this very promising and exciting field.

3. What do we know about the EHECR?

It is outside the scope of this review to present the full history of the cosmic ray detection and studies. This would cover the whole century (1912 is the year of the first decisive balloon experiments by Victor Hess). If we want a starting point for the genesis of the EHECR physics, we need to go back to the end of the thirties with the first observations of Pierre Auger and collaborators.[24] They studied the coincidence rates between counters with increasing separation (up to 150 m in their first experiments in Paris, more than 300 m when they repeated them at the Jungfraujoch in Switzerland). They inferred from this very modest measurement the existence of primary cosmic rays with energies as large as 1 PeV (10^{15} eV). Today's ground arrays used to detect the highest energy cosmic rays (some of them more than five orders of magnitude beyond the energies Auger considered as being extraordinary in his times) are actually based on this same technique, however sophisticated they may be: time coincidences between distant counters to identify a giant shower, and then the lateral profile of the densities of the particles hitting the counters to measure the total energy.

Figure 2 is a compilation[25] of the differential spectrum of cosmic ray flux as a function of energy. On this figure, integrated fluxes above three energy values are

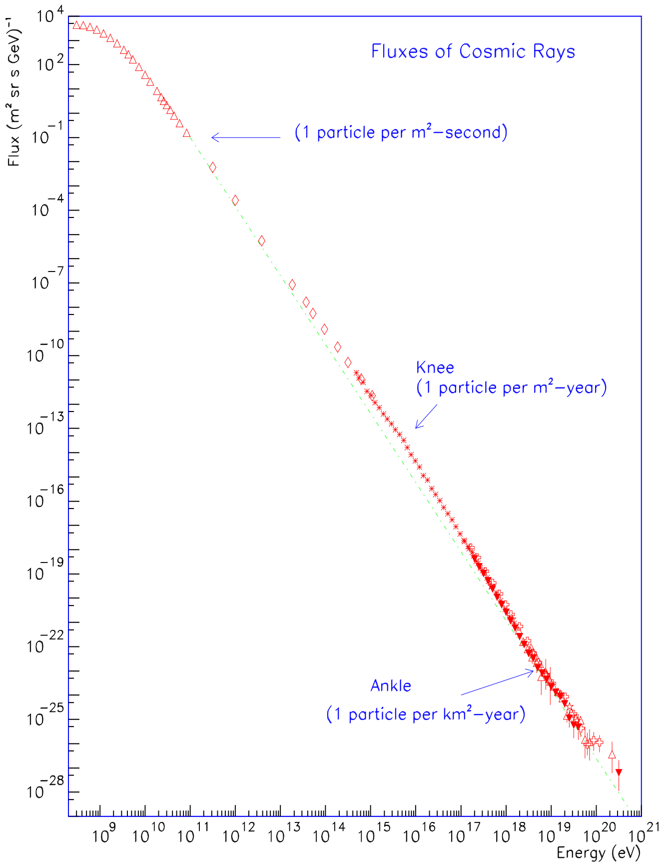

Fig. 2. The all-particle spectrum of cosmic rays.[25]

also indicated: 1 particle/m^2-second above 1 TeV, 1 particle/m^2-year above 10 PeV, 1 particle/km^2-year above 10 EeV. Ground detectors are the only alternative for the highest energy part of the spectrum.

In this section, and unless otherwise specified, we shall pay special attention to the events with energies exceeding 100 EeV. This value has no particular physical meaning except that it is well above the GZK cutoff.

Those events we are interested in (for brevity, let us call them 'Big Events') were observed in very small numbers over the past decades. After a review of the main experimental setups where their detection took place, we shall present a short overview of the information one can extract from the available data.

3.1. *Definitions*

The EAS detection performance of a ground based detector is given by its *acceptance* (or *aperture*) $\mathcal{A}$. For detectors large enough so that boundary effects can be neglected, it is assumed that at a given energy an EAS is detected whenever the shower axis hits the ground within an area S (for most cases the surface covered by the ground array) and with a zenith angle having a value between 0 (vertical showers) and a maximum $\theta_{\max}$, usually about $60°$. This maximum corresponds either to a loss of acceptance (like in ground arrays of thin scintillators) or to a change in the shower properties as for nearly horizontal showers the interaction point is usually far away from the detector and the shower is then mainly composed of fast muons.

The elementary *acceptance* for a solid angle $d\Omega$ in the direction θ is defined by:

$$d\mathcal{A} = S \cos\theta d\Omega$$

and the total geometrical aperture is:

$$\mathcal{A} = S \int_0^{\theta_{\max}} \cos\theta d\Omega = \pi S \sin^2\theta_{\max}$$

usually given in km^2sr units. One obtains the event rate by convoluting the aperture with the incident flux for a given type of particles. The geometrical aperture of an optical detector (like the Fly's Eye) should be multiplied by a reduction factor (of the order of 0.1) due to its duty cycle: such a detector can take data only during clear moonless nights. In the following, whenever we present the performance of a fluorescence detector, this factor will be included.

3.2. *Past and present detectors*

12 Big Events have been observed in the past[d] and, after thorough study, confirmed as having reached or exceeded the energy of 100 EeV. The corresponding detectors are listed below, with their total exposures in the relevant energy range.[26]

- **Volcano Ranch**[27] (New Mexico, USA). This is the first detector claiming to have detected a Big Event in February 1962. It was an array of 3 m^2 scintillator counters with a spacing of 900 m and a total area of about 8 km^2. The detector's total exposure was estimated to be of the order of 60 km^2 sr year.
- **Haverah Park**[20] (Great-Britain), an array of water Cerenkov tanks of various sizes and spacings covering an area of 12 km^2. The detector took data during almost 20 years (1968-1987) with a total exposure of 270 km^2 sr year. It reported 4 Big Events.
- **Fly's Eye**[28](Utah, USA), a binocular system of fluorescence telescopes. It is now being replaced by HiRes, a new generation fluorescence detector of larger aperture on the same site. Its total exposure is estimated at about 600 km^2 sr year in the mono-mode (an EAS detected only by one of the two telescopes) and 170 in the stereo-mode. The Fly's Eye detected the most energetic particle ever (320 EeV), but unfortunately in the mono-mode, hence with relatively large errors on the measurements of the incident direction and energy.

[d]We do not include here a few Big Events detected by the HiRes collaboration (see Section 5.1) not yet published.

- **AGASA**[21](Akeno, Japan), the largest, and still operating, ground array in the world. It is composed of 111 scintillator counters (2.2 m^2 surface and almost 1 km spacing) over an area of 100 km^2, with also 27 muon counters. AGASA has taken data since 1990, with a total exposure of 670 km^2 sr year. It reported up to now the detection of 7 Big Events, including the second in the energy hierarchy at 200 EeV.

Another detector (a combination of scintillators, muon and air-Cerenkov detectors), **Yakutsk**[29] (Russia), claims the detection of a Big Event. However, due to difficulties in estimating the exposure and energy resolution of this setup at the highest energies, their data are not included in the flux evaluations.

3.3. *The energy spectrum and flux*

The energy spectrum (Figure 2) ranges over 13 orders of magnitude in energy and 34 (!) orders of magnitude in flux. However, if one discards the saturation region at the lowest energies, the spectrum is surprisingly regular in shape. From the GeV energies to the GZK cutoff, it can be represented simply by three power-law curves interrupted by two breaks, the so-called "knee" and "ankle".

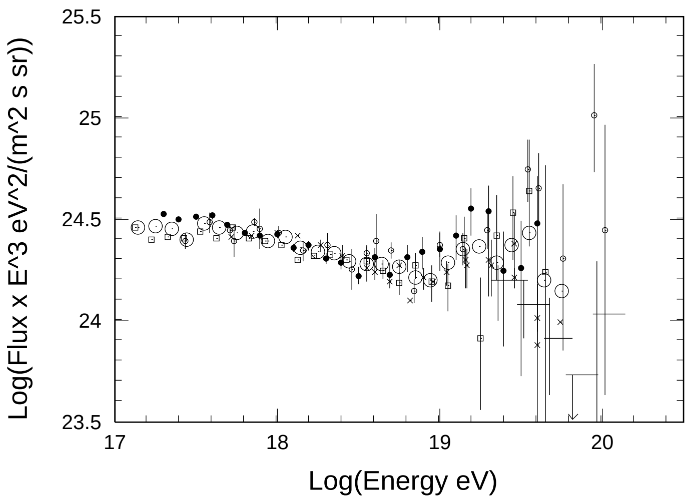

Fig. 3. Energy spectrum above 100 PeV. The compilation is from Ref.[21] updated by M.Nagano (private communication).

The supra-GZK events, and especially those above 100 EeV mentioned in the preceding section, were submitted to very close scrutiny, especially in the recent years where several dedicated projects were proposed to study this energy region. Their flux is extremely low. Figure 3 is a zoom on the highest energy range of the spectrum. On this figure, the energy spectrum is multiplied by E^3 so that the part below the EeV energies becomes flat. One can see the 'ankle' structure in its complexity: a steepening around the EeV and then a confused region where the GZK cutoff is expected. The ultimate data points come from very few events hence their large error bars, and due to normalization problems it is difficult to compare different experiments. On Figure 4 where the AGASA data alone are displayed,[31] one has a clearer view of what is expected (within a conventional framework) and what is observed. Here, the GZK cutoff is shown by the dashed line which is the expected

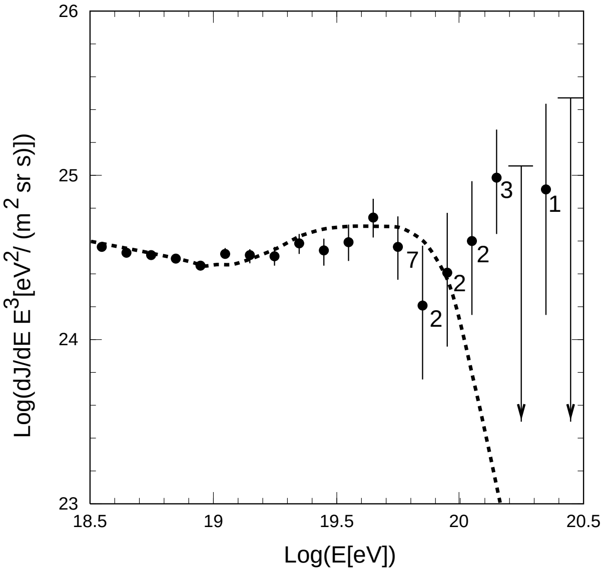

Fig. 4. Highest energy region of the cosmic ray spectrum as observed by the AGASA detector.[31] The figures near the data points indicate the number of events in the corresponding energy bin. The arrows show 90% confidence level upper limits. The dashed line is the expected spectrum if the sources were cosmologically distributed.

spectrum shape with the hypothesis of a cosmologically uniform distribution of the sources. The data suggests a change of slope as if a new phenomenon was rising above a steeply falling spectrum.

The flux of the highest energy cosmic rays obviously cannot be deduced from the data above the cutoff energies: no reliable fit to the spectrum shape is feasible in this region. A reasonable way of defining an order-of-magnitude flux is to base one's estimation on the total exposures mentioned above and the number of events observed. The exposure to events above the GZK cutoff for AGASA, Fly's Eye and Haverah Park detectors together, is of the order of 2000 km^2 sr yr. The number of events observed in this energy range over the lifetime of these detectors would yield an integrated flux which can be roughly parametrized by:

$$I(E > E_0) \approx \left(\frac{E_0}{10\,\mathrm{EeV}}\right)^{-2} \mathrm{km}^{-2}\mathrm{sr}^{-1}\mathrm{year}^{-1} \tag{1}$$

With $E_0 = 100$ EeV, the expected flux is 1 particle per km^2 per century! A statistically significant sample of events (necessary to reconstruct the shape of the spectrum, locate eventual point sources, study possible anisotropies in the incoming directions, and have hints on the chemical composition of the EHECR) cannot be obtained within a reasonable time unless the detectors have huge apertures. A typical and necessary order of magnitude would be 10^4 km^2 sr yr, ensuring a hundred events per year above 100 EeV and ten thousand above 10 EeV.

The GZK cutoff, as it would be expected if the sources are cosmologically distributed and if the observed cosmic rays have no exotic propagation and interaction properties, *is* violated. This statement, based on experimental data, can hardly be questioned. The next generation of detectors we will describe in Section 5 are designed to help us understand why and how.

3.4. *The chemical composition*

The methods to identify the primary cosmic ray from the EAS parameters were described in Section 2. One must keep in mind that observables contributing to the identification (depth of the shower maximum, muon to electron-photon ratio in the EAS at a given depth, position of the first interaction...) are subject to large fluctuations and each identity signature includes an unavoidable background. Therefore, the EHECR chemical composition is very likely to be unveiled only on a statistical basis, and by cross-checking the information deduced from as large a number of parameters as possible.

What we know at present on this issue is weak and controversial. The most recent information comes from the Fly's Eye and AGASA experiments. The Fly's Eye studies[28] (between 0.1 EeV and 10 EeV) are based on $X_{\max}$ behavior as a function of the logarithm of the primary energy. With this method, their data show evidence of a shift from a dominantly heavy composition (compatible with iron nuclei) to a light composition (protons), so that, if this interpretation is to be believed, the EHECR would mainly be protons.

The AGASA group based their primary identification on the muon content of the EAS at ground level,[32] an essentially independent method. Showers initiated by heavier nuclei are expected to have a higher muon content than light nuclei or protons, the gamma showers being the poorest in muons. Initially the conclusion of the AGASA experiment was quite opposite to the Fly's Eye: no change in chemical composition. However a recent critical review of both methods[33] showed that the inconsistencies were mainly due to the scaling assumption of the interaction model used by the AGASA group. The authors concluded that if a model with a higher (compared to the one given by scaling) rate of energy dissipation at high energy is assumed, as indicated by the direct $X_{\max}$ measurements of the Fly's Eye, both data sets demonstrate a change of composition, a shift from heavy (iron) at 0.1 EeV to light (proton) at 10 EeV. Different interaction models as long as they go beyond scaling, would lead to the same qualitative result but eventually with a different rate of change.

Gamma rays have also high cross sections with air and are still another possible candidate for EHECR but no evidence were found up to now for a gamma signature among the Big Events. The most energetic Fly's Eye event was studied in detail[34] and found incompatible with an electromagnetic shower. Both interpretations of the AGASA and the Fly's Eye data favor a hadronic origin.

3.5. *Distribution of the sources*

A necessary ingredient in the search for the origin of the EHECR is to locate their sources. This is done by reconstructing the incident cosmic ray's direction and checking if the data show images of point sources or correlations with distributions of astrophysical objects in our vicinity. Since a likely possibility as for the nature of the EHECR is that they are protons, we will say a few words about what we know of the galactic and extragalactic magnetic fields: this will show that for supra-GZK energies, proton astronomy is possible to some extent. We will then give a review of what we can extract from the present data in terms of anisotropy of the reconstructed directions and observed multiplets of events one may consider as images of point sources.

3.5.1. *Magnetic fields*

There are a limited number of methods to study the magnetic fields on galactic or extragalactic scales.[35] One is the measure of the Zeeman splitting of radio or maser lines in the interstellar gas. This method informs us mainly on the galactic magnetic fields, as extragalactic signals suffer Doppler smearing while the field values are at least three orders of magnitude below the galactic ones. The magnetic field structure of the galactic disc is therefore thought to be rather well understood. One of the parametrizations currently used is that of Vallée[36]: concentric field lines with a few μG strength and a field reversal at about one half of the disk radius. Outside the disk and in the halo, the field model is based on theoretical prejudice and represented by rapidly decreasing functions (e.g. gaussian outside the disk).

The study of extragalactic fields is mainly based on the Faraday rotation measure (FRM) of the linearly polarized radio sources. The rotation angle actually is a measurement of the integral of the function $n_e B_{||}$ where n_e is the electron/positron density and $B_{||}$ the longitudinal field component along the line of sight. Therefore, the FRM needs to be complemented by another measurement, namely that of n_e. This is done by observing the relative time delay versus frequency of waves emitted by a pulsar. Since the group velocity of the signal depends simultaneously on its frequency but also on the plasma frequency of the propagation medium, measurement of the dispersion of the observed signals gives an upper limit on the average density of electrons in the line of sight. Here again, because of the faintness of extragalactic signals, our knowledge of the strength and coherence distances of large scale extragalactic fields is quite weak and only upper limits over large distances can be extracted. An educated guess gives an upper limit of 1 nG for the field strength and coherence lengths of the order of 1 Mpc.[35]

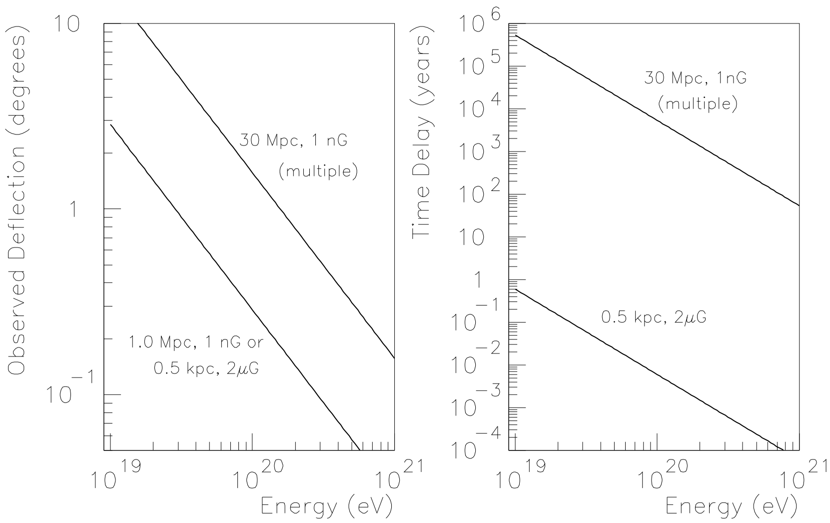

Fig. 5. Effect of magnetic fields on the propagation of a proton as a function of energy: angular deviation (left) and time delay (right), with respect to a straight line trajectory, in the framework of three realistic scenarios (see text).[37]

A few other more or less indirect methods exist for the study of large scale magnetic fields. *If* the EHECR are protons and *if* they come from point-like sources, the shape of the source image as a function of the cosmic ray energy will certainly be one of the most powerful of them. The Larmor radius R of a charged particle of charge Ze in kiloparsecs is given by:

$$R_{\rm kpc} \approx \frac{1}{Z}\left(\frac{E}{1\,{\rm EeV}}\right)\left(\frac{B}{1\,\mu{\rm G}}\right)^{-1}$$

The Larmor radius of a charged particle at 320 EeV is larger than the size of the galaxy if its charge is less than 8. If we take the currently accepted upper limit (10^{-9} G) for the extragalactic magnetic fields, a proton of the same energy should have a Larmor radius of 300 Mpc or more.

In Figure 5, three different situations are envisaged to evaluate the effects of magnetic fields on a high energy cosmic proton. The situations correspond to what is expected a-) for a trajectory through our galactic disk (0.5 kpc distance inside a 2 μG field) or b-) over a short distance (1 Mpc) through the extragalactic (1 nG) field (same curve), and finally c-) a 30 Mpc trajectory through extragalactic fields with a 1 Mpc coherence length (multiple scattering effect). One can see that at 100 EeV, the deviation in the third case would be about 2°. This gives an idea of the image size if the source is situated inside our local cluster or super-cluster of galaxies. Since the angular resolution of the (present and future) cosmic ray detectors can be comparable to or much better than this value, we expect to be able to locate the point-like sources (if they exist) or establish correlations with large-scale structures.

However, let us remember that this working hypothesis of very weak extragalactic magnetic fields is not universally accepted. Several authors recently advocated our bad knowledge of those fields showing that the arguments which will be developed in the following sections (the puzzling absence of correlations between the direction of the EHECR and either point sources or large structures) drop out if one envisages stronger magnetic fields (typically at the μG level) either locally[38] or distributed over larger, cosmological, scales.[39]

3.5.2. *Anisotropies*

In the search for potential sources, the propagation arguments incite us to look

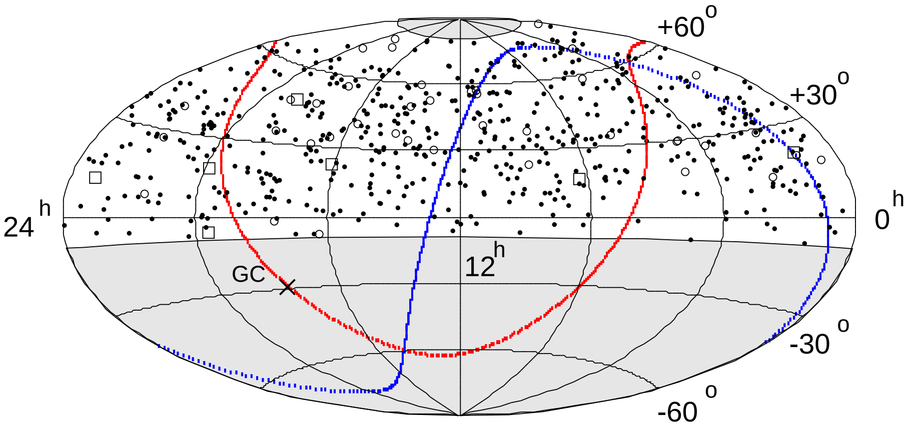

Fig. 6. Arrival directions of cosmic rays with energies above 10 EeV (equatorial coordinates), as measured by the AGASA experiment.[40] The thick dotted lines show the galactic and supergalactic planes (GC indicating the galactic center). The shaded regions are those invisible to the AGASA detector. See text.

for correlations with the distribution of astrophysical matter within a few tens of Mpc. In our neighborhood, there are two structures showing an accumulation of objects, both only partially visible from any hemisphere: the galactic disk on a small scale and the supergalactic plane on a large scale, a structure roughly normal to the galactic plane, extending to distances up to $z \approx 0.02$ (about 100 Mpc) and correlated with a denser distribution of radio galaxies. In equatorial coordinates with the hypothesis of an isotropic distribution of the sources, and over large periods of data taking, the right ascension distribution of events must be uniform and the declination distribution can be parametrized with the known zenith angle dependence of the detector aperture.

The most recent analysis on the correlation between arrival directions and possible source locations was done by the AGASA experiment for the highest energy range.[40] The analysis is based on 581 events above 10 EeV, a subset of 47 events above 40 EeV and 7 above 100 EeV. Figure 6 is a compilation of the total sample in equatorial coordinates. The dots, circles and squares are respectively events with energies above 10, 40 and 100 EeV. The data show no deviation from the expected uniform right ascension distribution. An excess of 2.5 σ is found at a declination of 35° and can be interpreted as a result of observed clusters of events (see below). No convincing deviation from isotropy is found when the analysis is performed in galactic coordinates.

The same collaboration[41] made also a similar analysis for the lower energy region (events down to 1 EeV and detected with zenith angles up to 60°). In this article, a slight effect of excess events in the direction of the galactic center was announced. A similar study[42] with the Fly's Eye data, concludes on a small correlation with the galactic plane for events with energies lower than 3.2 EeV and isotropy for higher energies.

In summary, both the AGASA and Fly's Eye experiments seem to converge on some anisotropy in the EeV range (correlation with the galactic plane and center) and isotropy above a few tens of EeV. This result may seem surprising - one naively expects the correlations to be stronger when the cosmic rays have large magnetic rigidity. It is actually explained by the fact that the low energy component may be dominantly galactic heavy nuclei (see the section on chemical composition), hence a (weak) correlation with the galactic plane, whereas the higher energy cosmic rays would be dominated by extragalactic protons.

With the present data it is difficult to come to any clear conclusion on the anisotropy issues, especially at the highest energies. All we can do is acknowledge the problems and make a list of technical requirements to solve them. First of all, and whatever the analysis methods used, statistics is the sinews of war. One needs at least an order of magnitude in the rate with which we are detecting the relevant events in the highest energy range, hence in the collecting detectors' aperture. This is the principal aim of the next generation of experiments. Second, the powerful harmonic analysis needs full sky coverage and, as much as possible, uniform exposure. This means data from both hemispheres. All the data used in the above analyses come from the northern hemisphere. Possible correlations with the galactic plane or the galactic center will only be confirmed, or invalidated, if a detector systematically explores the southern sky. Also, due to day-night effects, a fluorescence detector does not have a uniform right-ascension coverage. One should also take into account the angular acceptance. The scintillator technique (used in the AGASA detector) has an intrinsic limitation for large angles. The use of Cerenkov tanks (as in the Haverah Park experiment) circumvents this limitation: it can even detect horizontal showers with equal efficiency, although the bending of the charged particles of the shower makes the analysis more difficult for large angles. All these constraints have been carefully considered in the design of the next generation experiments.

3.5.3. *Point sources?*

If the sources of EHECR are nearby astrophysical objects and if, as expected, they are in small numbers, a selection of the events with the largest magnetic rigidity would combine into multiplets or clusters which would indicate the direction to look for an optical or radio counterpart. Such an analysis was done systematically by the AGASA group.[40] Figure 7 shows the subsample of events in the AGASA

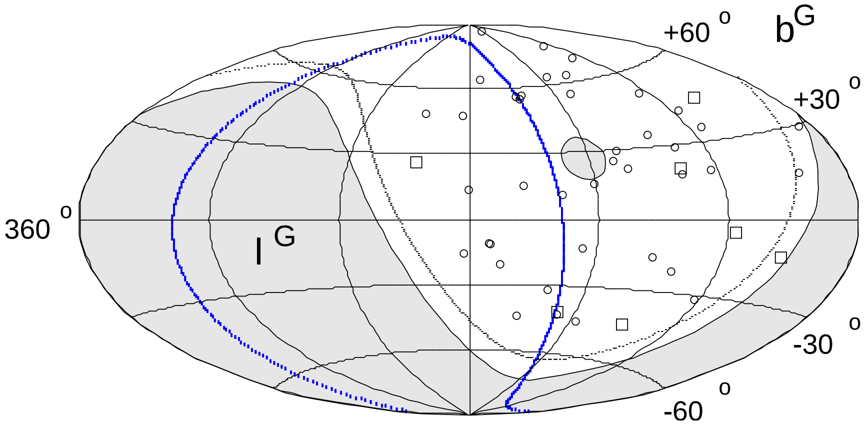

Fig. 7. Arrival directions of cosmic rays with energies above 40 EeV (galactic coordinates), as measured by the AGASA experiment.[40] See text.

catalog with energies in excess of 100 EeV (squares) and in the range 40-100 EeV (circles). A multiplet is defined as a group of events whose error boxes (2.5° circles) overlap. One can see that there are three doublets and one triplet. If one adds the Haverah Park events, the most southern doublet also becomes a triplet. The chance probability of having as many multiplets as observed with a uniform distribution are estimated by the authors to less than 1%.[e]

A search for nearby astrophysical objects within an angle of 4° from any event in a multiplet was also done, and produced a few objects. One of the most interesting candidates is Mrk 40, a galaxy collision, since the shock waves generated in such phenomena are considered by some authors[43] as being valid accelerating sites.

Another way of using the observed multiplets, *assuming* that they come from an extragalactic point source, is to consider the galactic disk as a magnetic spectrometer which can give information on the charge of the incident cosmic rays. Cronin[44] made such an analysis on the doublet where the energy difference between the two events is the largest (a factor of four). He uses the magnetic field model of Vallée[36] to trace back the detected couple of events outside of the galaxy assuming various charges. It is shown that the maximum charge compatible with a separation less than the detector's angular resolution is 2 for the members of the doublet with conservative integrated values for the magnetic field, a result compatible with protons being the most likely EHECR.

3.5.4. *Is a galactic origin possible?*

One can put forward at least three reasons to argue for an extragalactic origin of

[e] The chance probability is very difficult to evaluate in an *a posteriori* analysis and depends strongly on the assumed experimental error box size.

the EHECR sources:

1. The galactic size and magnetic fields are such that the EHECR cannot be confined inside the galaxy;
2. One usually assumes that there are no likely astrophysical objects which can be considered as remarkable accelerators inside our galaxy;
3. *If* the accelerated particles are light nuclei, their direction should show correlations with the galactic plane, which is not the case.

The second argument was sometimes challenged in the past by authors who propose some galactic objects such as microquasars and pulsars as possible powerful accelerating engines. None of these ideas seem to us fully convincing, in the sense that they are generally based on *ad hoc* hypotheses and fail to explain the full set of observational data on the EHECR (see e.g. Blanford[45] for a recent review).

4. Possible sources of the EHECR

Today's understanding of the phenomena responsible for the production of EHERC, i.e. the transfer of macroscopic amounts of energy to microscopic particles, is still limited. One distinguishes two classes of processes: the so called "Top-Down" and "Bottom-Up" scenarios. In the former, the cosmic ray is one of the stable decay products of a super-massive particle. Such particles with masses exceeding 1 ZeV can either be meta-stable relics of some primordial field or highly unstable particles produced by the radiation, interaction or collapse of topological defects. Those processes are reviewed in Section 4.3

In the second scenario discussed in section 4.2 the energy is transferred to the cosmic rays through their interaction with electromagnetic fields. This classical approach does not require new physics as opposed to the "Top-Down" mechanism, but does not exclude it either since, in some models, the accelerated particle - the cosmic ray - is itself "exotic".

Once accelerated the cosmic rays must propagate from their source to the observer. At energies above 10 EeV and except for neutrinos, the Universe is not transparent to ordinary stable particles on scales much larger than about 10 Mpc. Regardless of their nature, cosmic rays lose energy in their interaction with the various photon backgrounds, dominantly the copious Cosmic Microwave Background (CMB) but also the Infra-Red/Optical (IR/O) and the Radio backgrounds. The GZK cutoff puts severe constraints on the distance that a cosmic ray can travel before losing most of its energy or being absorbed. The absence of prominent visible astrophysical objects in the direction of the observed highest energy cosmic rays together with this distance cutoff adds even more constraints on the "classical" Bottom-Up picture.

It is beyond the scope of this review to describe all the scenarios - they are far too numerous - proposed for the production of the EHECR. Let us simply agree on the fact that the profusion of models shows that none of them is totally satisfactory.

Consequently we will try to present, from an experimentalist's point of view, the main features of the various categories of models. We will also try to focus on the possible experimental constraints, if they exist, or on the problems related to the EHECR and which remain unanswered. For a more detailed review we urge the reader to consult the excellent report by P.Bhattacharjee and G.Sigl[46] and the references therein. Extensive use of this report is made in some of the following sections where we avoided repeated reference to it.

At first sight, it would seem natural to discuss potential sources and acceleration mechanisms before the description of the cosmic ray transportation to Earth. However, and because the attenuation or interaction lengths are relatively short and strongly energy dependent in the range of interest, the observed spectra do not only depend on the nature of the sources but also on their distribution. In addition, the GZK cutoff puts important constraints which we prefer to discuss before describing the possible nature of the sources themselves.

4.1. *Propagation*

We will focus here on the propagation of atomic nuclei (in particular protons) and photons. Electrons are not considered as potential EHECR because they radiate most of their energy while crossing the cosmic magnetic fields. Among the known stable particles, and within the framework of the Standard Model, those are the only possible candidates for EHECR. As we mentioned in Section 3.4, the actual data effectively favor a hadronic composition.

Neutrinos and the lightest super-symmetric particles (LSP) should deserve special attention as they may travel through space unaffected even on large distances. However, for neutrinos the interaction should occur uniformly in atmospheric depth, a feature which is not reproduced by the current data. While neutrinos may very well be one of the components of the high energy end of the cosmic ray spectrum and prove to be an unambiguous signature of the new physics underlying the production mechanisms (see below) they do not seem to dominate the observations at least up to energies of a few 10^{20} eV.

The LSP are expected to have smaller interaction cross sections with photons and a higher threshold for pion photo-production due to their higher mass (see Eq. (2) below). Therefore they may travel unaffected by the CMB on distances 10 to 30 times larger than nucleons. However in usual models the LSP is neutral and cannot be accelerated in a Bottom-Up scenario and must be produced as a secondary of an accelerated charged particle (e.g. protons). This accelerated particle must reach energies at least one order of magnitude larger than the detected energy (order of ZeV) and will produce photons. The acceleration site should therefore be detectable as a very powerful gamma source in the GeV range. In a Top-Down scenario including Super-Symmetry, the problem of propagation is of somewhat lesser importance as the decaying super-massive particles may be distributed on cosmological or on nearby scales and are, in any case, invisible (see Section 4.3). Finally let us stress that the analysis of the EHECR shower shape limits the mass of the cosmic ray to about 50 GeV,[47] an additional constraint for the LSP candidate.

4.1.1. *Protons and Nuclei: The GZK cutoff*

The Greisen-Zatsepin-Kuzmin (GZK) cutoff (see Section 1) threshold for collisions between the cosmic microwave background (CMB) and protons (photo-pion production) can be expressed in the CMB "rest" frame as

$$E_{th} \simeq \frac{E_\gamma m_p}{2\epsilon} \sim \frac{7 \times 10^{16}}{\epsilon} \tag{2}$$

where ϵ is the target photon energy and E_{th} the proton threshold, both in electron-volts. For an energetic CMB photon with $\epsilon = 10^{-3}$ eV, E_{th} is $7{\times}10^{19}$ eV which is where one expects the GZK cutoff to start.

The interaction length for this process can be estimated from the photo-pion cross section (taken beyond the Δ resonance production) and the CMB photon density:

$$L = (\sigma\rho)^{-1} \simeq 1.7 \times 10^{25}\,\mathrm{cm} \simeq 6\,\mathrm{Mpc}$$

for $\rho = 410\,\mathrm{cm}^{-3}$ and $\sigma = 135$ μbarns.

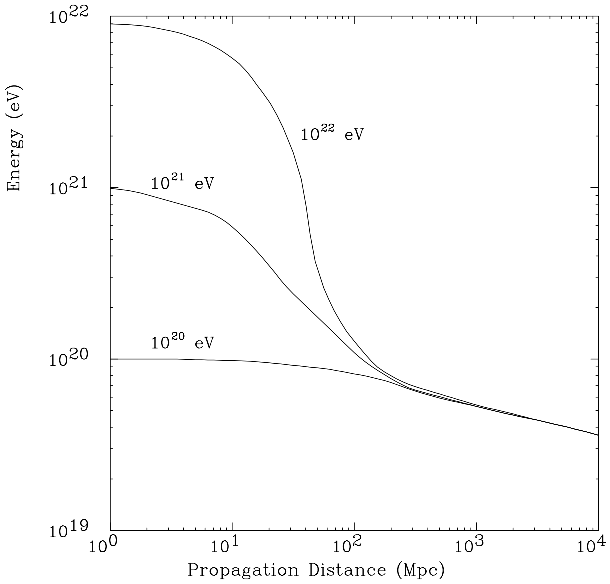

Fig. 8. Energy of a proton as a function of the propagation distance through the 2.7K cosmic background radiation for various initial energies.[37]

The energy loss of protons of various initial energies as a function of the propagation distance is shown in Figure 8. Above 100 Mpc the observed energy is below 10^{20} eV regardless of its initial value. One should point out that this reduction is not the consequence of a single catastrophic process but of many collisions (more than 10) each of which reduces the incident energy by 10 to 20%. Therefore the probability to travel without losses is negligible.

A proton may also produce e^+e^- pairs on the CMB at a much lower threshold (around 5×10^{17} eV) but the cross section is orders of magnitude smaller and together with a smaller inelasticity the overall interaction length stays around 1 Gpc.

For nuclei the situation is in general more difficult. They undergo photo-disintegration in the CMB and infrared radiations losing on average 3 to 4 nucleons per Mpc when their energy exceeds 2×10^{19} eV to 2×10^{20} eV depending on the IR background density value. The IR background is much less well known than the CMB and the attenuation length (see Figure 9) derived for nuclei must be taken with precaution.

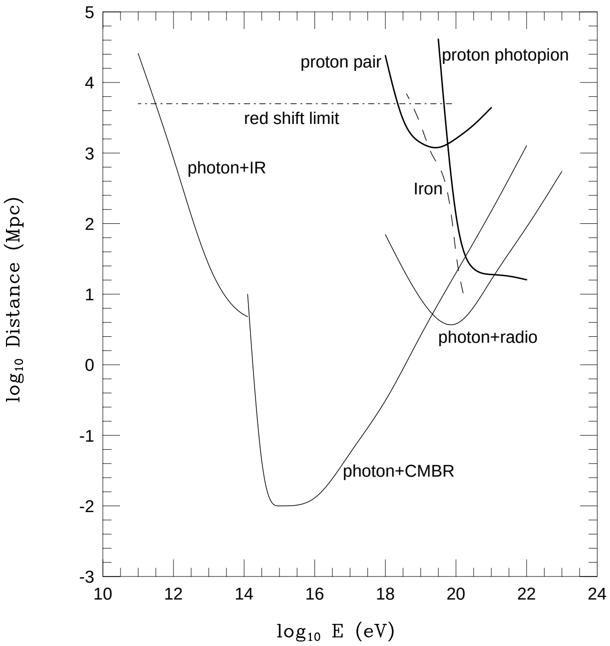

Fig. 9. Attenuation length of photons, protons and iron in various background radiations as a function of energy.[37] The dot-dashed line represents the absolute upper limit on the distance a particle can travel toward Earth, regardless of its initial energy.

4.1.2. *Electrons and Photons: Electromagnetic Cascades*

Top-Down production mechanisms predict that, at the source, photons (and neutrinos) dominate over ordinary hadrons by about a factor of ten. An observed dominance of gammas in the supra-GZK range would then be an almost inescapable signature of a super-heavy particle decay. Photons are also secondaries of more ordinary processes such as photo-pion production; their propagation is thus worth studying. Unlike photons, electrons and positrons cannot constitute the primary CR as the radiation energy losses they undergo forbid them to reach the highest energies by many orders of magnitude.

High energy photons traveling through the Universe produce e^+e^- pairs when colliding with the Infra-Red/Optical (IR/O), CMB or Universal Radio Background (URB) photons. As can be seen on Figure 9 the attenuation length gets below 100 Mpc for photon energies between 3×10^{12} eV and 10^{22} eV. In this energy range, nearly 10 orders of magnitude, the Universe is opaque to photons on cosmological scales.

Once converted, the e^+e^- pair will in turn produce photons mostly via Inverse Compton Scattering (ICS) (the case of synchrotron radiation, usually non dominant, will be treated in the next section). At our energies, those two dominant processes are responsible for the production of electromagnetic (EM) cascades.

Much above the pair production threshold ($s \gg 4m_e^2$, where $\sqrt{s}$ is the CM energy) the ICS ($\sigma_{\rm ICS}$) and the pair production ($\sigma_{\rm pp}$) cross sections are related by :

$$\sigma_{\rm pp} \approx 2\sigma_{\rm ICS} = \frac{3}{2}\sigma_T \frac{m_e^2}{s} \log\left(\frac{s}{2m_e^2}\right)$$

where m_e is the electron mass and $\sigma_T = 8\pi\alpha^2/3m_e^2 = 665$ mbarn the Thomson cross section of photon elastic scattering on an electron at rest. The $1/s$ dependence implies that far from the pair threshold the EM cascade develops slowly as it is the case when the initial photon energy is above 10^{22} eV.

At the pair production threshold ($s \sim 4m_e^2$), the pair cross section reaches a value of ~ 170 mbarn and $\sigma_{\rm ICS}$ is nearly equal to the Thomson cross section. The EM cascades develop very rapidly. From Figure 9 one sees that at the pair production threshold against the CMB photons (2×10^{14} eV) conversion occurs on distances of about 10 kpc (a thousand times smaller than for protons at GZK energies) while subsequent ICS of electrons on the CMB in the Thomson regime will occur on even smaller scales (1 kpc).

As a consequence, all photons of high energy (but below 10^{22} eV) will produce, through successive collisions on the various photon backgrounds (URB, CMB, IR/O), lower and lower energy cascades and pile up in the form of a diffuse photon background below 10^{12} eV with a typical $\alpha = 1.5$ power law spectrum. This is a very important fact as measurements of the diffuse gamma ray background in the 10^7-10^{11} eV range done for example by EGRET[48] will impose limits on the photon production fluxes of Top-Down mechanisms and consequently on the abundance of topological defects or relic super-heavy particles.

4.1.3. *Charged Particles: Magnetic Fields*

The effect of magnetic fields (galactic or extragalactic) on the deflection of charged particles has been reviewed in Section 3.5.1. Here we will present some of the effects of the fields on EM cascade production.

Electrons and positrons produced through EM cascades lose energy via synchrotron radiation at a rate given by:

$$-\frac{dE}{dt} = \frac{4\alpha^2}{3m_e^2} B^2 \left(\frac{E}{m_e}\right)^2,$$

where we assume a random field B isotropically distributed with respect to the electron direction.

At high enough energy, i.e.

$$E \sim \left(\frac{B}{10^{-9}\,\mathrm{G}}\right)^{-1} 10^{19}\,\mathrm{eV}$$

this process will dominate over ICS on URB or CMB photons. The above threshold is not very strict as it depends on the URB density which is not a very well known quantity. The emitted gammas have a typical energy given by[46]

$$E_{\mathrm{synch}} = 6.3 \times 10^{11} \left(\frac{E}{10^{19}\,\mathrm{eV}}\right) \left(\frac{B}{10^{-9}\,\mathrm{G}}\right) \mathrm{eV}.$$

Again low energy photon flux measurements will put constraints on the extragalactic fields and/or on the initial photon flux.

Above threshold, the synchrotron radiation will damp the electron-positron pair energy extremely quickly. At 100 EeV in a 10^{-9} G magnetic field the attenuation length is of the order of 20 kpc. If one observes gammas above 10^{20} eV they could not be high energy secondaries (e.g. from ICS) of an even higher energy photon converted into a pair. They must instead be primary ones. Consequently, their flux $j_\gamma(E)$ per unit area and unit solid angle at a given energy is directly related to the source distribution without any transport nor cosmological effects in between :

$$j_\gamma(E) \sim \frac{1}{4\pi} l_\gamma(E)\phi(E)$$

where $\phi(E)$ is the source emission density per unit time and energy interval and $l_\gamma(E)$ is the photon interaction length.

Of course quantitative predictions of such effects is pending definite measurements of the galactic and extragalactic magnetic fields. Although the magnetic fields of the galactic disc are now believed to be fairly well known this is not the case of the ones in the halo or extragalactic media. As mentioned in Section 3.5.1, several authors advocate our bad knowledge of those fields in explaining the puzzling observational data and question both the typical value of 10^{-9} G and the coherence length of 1 Mpc usually assumed for the extragalactic fields.[49]

4.2. *Conventional acceleration: Bottom-Up scenarios*

One essentially distinguishes two types of acceleration mechanisms:

- Direct, one-shot acceleration by very high electric fields. This occurs in or near very compact objects such as highly magnetized neutron stars or the accretion disks of black holes. However, this type of mechanism does not naturally provide a power-law spectrum.

- Diffusive, stochastic shock acceleration in magnetized plasma clouds which generally occurs in all systems where shock waves are present such as supernova remnants or radio galaxy hot spots. This statistical acceleration is known as the Fermi mechanism of first (or second) order, depending on whether the energy gain is proportional to the first (or second) power of β, the shock velocity.

Extensive reviews of acceleration mechanisms exist in the literature, e.g. on acceleration by neutron stars,[50] shock acceleration and propagation,[52] non relativistic shocks,[53] and relativistic shocks.[54]

Hillas has shown[55] that irrespective of the details of the acceleration mechanisms, the maximum energy of a particle of charge Ze within a given site of size R is:

$$E_{\rm max} \approx \beta Z \left(\frac{B}{1\,\mu{\rm G}}\right)\left(\frac{R}{1\,{\rm kpc}}\right) 10^{18}\ {\rm eV} \tag{3}$$

where B is the magnetic field inside the acceleration volume and β the velocity of the shock wave or the efficiency of the acceleration mechanism. This condition essentially states that the Larmor radius of the accelerated particle must be smaller than the size of the acceleration region, and is nicely represented in the Hillas diagram shown in Figure 10.

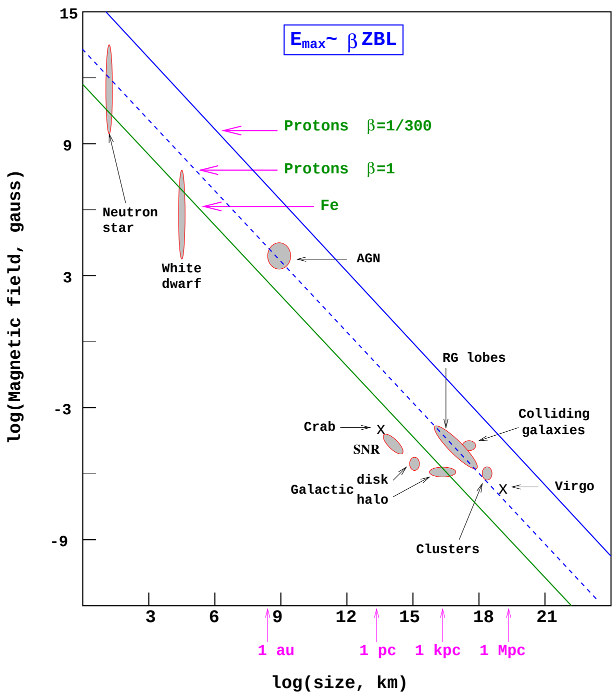

Fig. 10. Size and magnetic field strength of possible acceleration sites. Objects below the diagonal lines cannot accelerate the corresponding elements (Iron with β = 1 or protons β = 1 and β = 1/300) above 10^{20} eV.

4.2.1. *Candidate sites*

Inspecting the Hillas diagram one sees that only a few astrophysical sources satisfy the necessary, but not sufficient, condition given by Eq. (3). Some of them are reviewed e.g. by Biermann.[56] Let us just mention, among the possible candidates, pulsars, Active Galactic Nuclei (AGN) and Fanaroff-Riley Class II (FR-II) radio galaxies.

Pulsars
From a dimensional analysis, the electric field potential drop in a rotating magnetic pulsar is given by:

$$\Delta\Phi = \frac{B \times R^2}{\Delta T} \tag{4}$$

One obtains $e\Delta\Phi = 100$ EeV with $B = 10^9\,\mathrm{T}$, $\Delta T = 10^{-3}\,\mathrm{s}$ and $R = 10^4\,\mathrm{m}$. However the high radiation density in the vicinity of the pulsar will produce e^+e^- pairs from conversion in the intense magnetic field.[50] These pairs will drift in opposite directions along the field lines and short circuit the potential drop down to values of about 10^{13} eV. Moreover in the above dimensional analysis a perfect geometry is assumed. Actually, a more realistic geometry would introduce an additional factor $R/c\Delta T \sim 0.1$, and further decrease the initial estimate. Finally, as will be described in the next section, synchrotron radiation losses in such compact systems become very important even for protons.

AGN cores and jets
Blast wave in AGN jets have typical sizes of a few percent of a parsec with magnetic fields of the order of 5 gauss.[51] They could in principle lead to a maximum energy of a few tens of EeV. Similarily for AGN cores with a size of a few 10^{-5} pc and a field of order 10^3 G one reaches a few tens of EeV. However those maxima, already marginal, are unlikely to be achieved under realistic conditions. The very high radiation fields in and around the central engine of an AGN will interact with the accelerated protons producing pions and e^+e^- pairs. Additional energy loss due to synchrotron radiation and Compton processes lead to a maximum energy of about 10^{16} eV, way below the initial value.[46] To get around this problem, the acceleration site must be away from the active center and in a region with a lower radiation density such as in the terminal shock sites of the jets: a requirement possibly fulfilled by FR-II radio galaxies.

FR-II radio galaxies
Radio-loud quasars are characterized by a very powerful central engine ejecting matter along thin extended jets. At the ends of those jets,

the so-called hot spots, the relativistic shock wave is believed to be able to accelerate particles up to ZeV energies. This estimate depends strongly on the value assumed for the spots' local magnetic field, a very uncertain parameter. Nevertheless FR-II galaxies seem the best potential astrophysical source of EHECR.[56] Unfortunately, no nearby (less than 100 Mpc) object of this type is visible in the direction of the observed highest energy events. The closest FR-II source, actually in the direction of the Fly's Eye event at 320 EeV, is at about 2.5 Gpc, way beyond the GZK distance cuts for nuclei, protons or photons.

4.2.2. *Additional constraints*

In addition to the constraint given by Eq. (3), candidate sites must also satisfy two additional conditions.

- The acceleration must occur on a reasonable time scale, e.g. the size of the acceleration region must be less than the interaction length of the accelerated particle. This is a relatively weak constraint since all the objects in the Hillas diagram have a size below 1 Mpc. However, in shock acceleration mechanisms the rate of energy loss on the CMB must be less than the rate of energy gain:

$$-\frac{dE_{\text{loss}}}{dt} \propto \text{const} \times E < \frac{dE_{\text{gain}}}{dt} \tag{5}$$

- The acceleration region must be large enough so that synchrotron losses are negligible compared to the energy given by Eq. (3). For shock acceleration the radiated synchrotron power must be below the rate of energy gain:

$$-\frac{dE_{\text{sync}}}{dt} \propto \frac{E^4}{R^2} \propto B^2 \ E^2 \tag{6}$$

Using, as the characteristic acceleration time, $T_A = R/\beta$ (where β is the shock velocity) one finds a characteristic gain rate of :

$$\frac{dE_{\text{gain}}}{dt} \approx \frac{E_{\max}}{T_A} \propto \beta^2 \ B. \tag{7}$$

For a given $E_{\max}$ (e.g. 100 EeV), these two constraints define two lines in the $\log B$, $\log \beta$ plane above and below which particles cannot be accelerated at the required energy. As can be seen on Figure 11 the only remaining candidates are the radio galaxy hot spots (RGH).

To conclude on the bottom-up scenario, let us mention a recent analysis from Farrar and Biermann.[57] They have shown that, on cosmological scales, the correlation between the arrival direction of the five highest energy events and Compact Quasi Stellar Objects (CQSO's) which include radio-loud galaxies is unlikely to be accidental. They calculate the chance alignment probability to be 5×10^{-3}. Only a

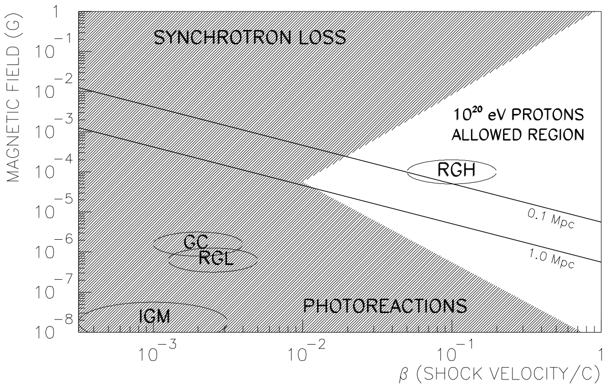

Fig. 11. Magnetic field strength and shock velocity of possible sites. GC refers to Galactic Cluster (accretion shocks), IGM to Inter Galactic Medium, RGL to Radio Galaxy Lobes and RGH to Radio Galaxy Hot Spots (a subclass of RGL).[37]

new type of neutral particle could travel on distances over 1 Gpc without losing its energy on the CMB nor being deflected by extragalactic magnetic fields. More data at very high energy are needed to validate this result which would sign the existence of a new particle physics phenomenon.

4.3. *"Exotic" sources: Top-Down scenario*

One way to overcome the many problems related to the acceleration of EHECR, their flux, the visibility of their sources and so on, is to introduce a new unstable or meta-stable super-massive particle, currently called the X-particle. The decay of the X-particle produces, among other things, quarks and leptons. The quarks hadronize, producing jets of hadrons which, together with the decay products of the unstable leptons, result in a large cascade of energetic photons, neutrinos and light leptons with a small fraction of protons and neutrons, part of which become the EHECR.

For this scenario to be observable three conditions must be met:

- The decay must have occurred recently since the decay products must have traveled less than about 100 Mpc because of the attenuation processes discussed above.
- The mass of this new particle must be well above the observed highest energy (100 EeV range), a hypothesis well satisfied by Grand Unification Theories (GUT) whose scale is around 10^{24}-10^{25} eV.
- The ratio of the volume density of this particle to its decay time must be compatible with the observed flux of EHECR.

The X-particles may be produced by way of two distinct mechanisms:

- Radiation, interaction or collapse of Topological Defects (TD), producing X-particles that decay instantly. In those models the TD are leftovers from the GUT symmetry breaking phase transition in the very early universe. However very little is known on the phase transition itself and on the TD density that survives a possible inflationary phase, and quantitative predictions are usually quite difficult to rely on.
- Super-massive metastable relic particles from some primordial quantum field, produced after the now commonly accepted inflationary stage of our Universe. Lifetime of those relics should be of the order of the age of the universe and must be guaranteed by some almost conserved protecting symmetry. It is worth noting that in some of those scenarios the relic particles may also act as non-thermal Dark Matter.

In the first case the X-particles instantly decay and the flux of EHECR is related to their production rate given by the density of TD and their radiation, collapse or interaction rate, while in the second case the flux is driven by the ratio of the density of the relics over their lifetime. In the following the terms *"production or decay rate"* will refer to these two situations. Before discussing the exact nature of the X-particles we shall briefly review the main characteristics of the decay chain and the expected flux of the energetic outgoing particles.

4.3.1. *Xdecay and secondary fluxes*

At GUT energies and if they exist, squark and sleptons are believed to behave like their corresponding super-symmetric partners so that the gross characteristics of the cascade may be inferred from the known evolution of the quarks and leptons. Of course the internal mechanisms of the decay and the detailed dynamics of the first secondaries do depend on the exact nature of the particles but the bulk flow of outgoing particles is most certainly independent of such details.[46]

A common picture for the hadronisation of the decay products follows three steps. At the high energy end, the perturbative QCD expansion provides a good description of the hard processes driving the dynamics of the parton cascade. At a cutoff energy of about 1 GeV soft processes become dominant and partons are glued together to form color singlets which will in turn decay into known hadrons. The LUND[58] string fragmentation model provides a description for the second and last phases while a model like the Local Parton-Hadron Duality directly relates the parton density in the parton cascade to the final hadron density.[59] Nevertheless and despite the fact that up to 40% of the initial energy may turn into LSP, the cascade produces a rather hard[f] hadron spectrum adequately described by:

$$\frac{dN_h}{dE} \propto E^{-\alpha} \quad \text{with} \quad 1 < \alpha < 2$$

[f]For a power law spectrum of exponent $\alpha < 2$ the total energy ($\propto E^{2-\alpha}$) is dominated by the high energy end of the integral, i.e. a few very energetic particles, thus a hard spectrum, while for $\alpha > 2$ the energy is carried by the very large number of low energy particles, i.e. a soft spectrum.

in the range $E/m_X \ll 1$, where m_X is the X-particle mass. At the high energy end a cutoff occurs at a value depending on the X-particle mass and on the eventual existence of new physics such as Super Symmetry (SUSY), which would displace the maximum of the hadron spectrum to a lower energy (see Figure 12).

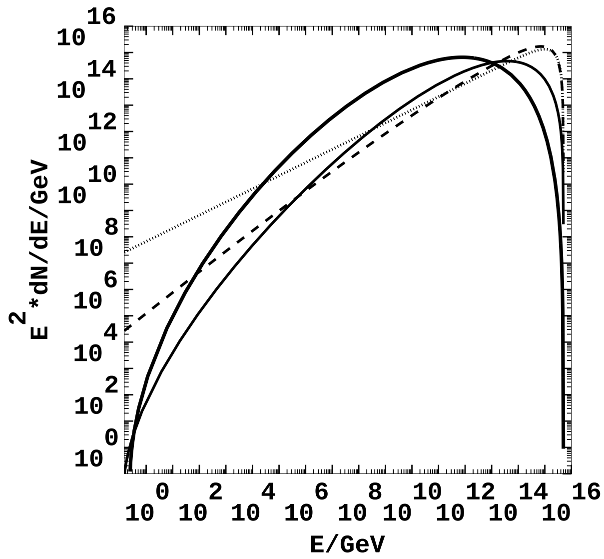

Fig. 12. Fragmentation function in the Modified Leading Log Approximation for a total jet energy of 5×10^{24} eV with SUSY (thick solid line peaking at 10^{12}GeV) and without SUSY (thin solid Line) as calculated by Bhattacharjee and Sigl.[46] Other lines (dashed and dotted) are older approximated expressions.

Indeed, Super Symmetry is not the only possible candidate theory for new physics beyond the standard model: other (yet unknown) models may appear as possible alternatives in the future. However, in all cases, secondaries from Top-Down mechanisms should manifest themselves as a change of slope in the EHECR spectrum, above 10 EeV and over a range which will reflect the (new) physics at play.

In all conceivable Top-Down scenarios, photons and neutrinos dominate at the end of the hadronic cascade. This is *the* important distinction from the conventional acceleration mechanisms. The spectra of photons and neutrinos can be derived from the charged and neutral pion densities in the jets as:

$$\Phi_\gamma^{\pi^0}(E,t) \simeq 2\int_E^{E_{\rm jet}} \Phi_{\pi^0}(\varepsilon,t)d\varepsilon/\varepsilon$$

$$\Phi_\nu^{\pi^\pm}(E,t) \simeq 2.34\int_{2.34E}^{E_{\rm jet}} \Phi_{\pi^\pm}(\varepsilon,t)d\varepsilon/\varepsilon$$

where $E_{\rm jet}$ is the total energy of the jet (or equivalently the initial parton energy). Since $\Phi_{\pi^\pm}(\varepsilon,t) \simeq 2\Phi_{\pi^0}(\varepsilon,t)$, photons and neutrinos should have very similar spectra. These injection spectra must then be convoluted with the transport phenomena to obtain the corresponding flux on Earth. As was mentioned in Section 4.1.2 the photon transport equation strongly depends on its energy and on the badly known Universal Radio Background and extragalactic magnetic fields.

4.3.2. *X production or decay rates: a lower limit*

The production or decay rates of the X-particles are very model dependent and no firm prediction on the expected flux of EHECR can be made. However, in their review, Bhattacharjee and Sigl evaluate with a simple model the rate needed to explain the observed EHECR fluxes. Assuming that photons dominate at the source and on Earth and that they follow a power law spectrum of index α; assuming also that the initial X decay secondaries are quarks and leptons in equal numbers, they calculate a lower limit on the production rate given by (for $\alpha = 1.5$):

$$\dot{n}_X \geq 10^{-46} \left(\frac{10\,\mathrm{Mpc}}{l_E(E_\gamma)}\right) \left(\frac{E^2 j_\gamma(E)}{\mathcal{F}_\oplus}\right) \sqrt{\frac{m_X}{10^{16}\,\mathrm{GeV}}}\ \mathrm{cm}^{-3}\mathrm{s}^{-1} \tag{8}$$

Here $\mathcal{F}_\oplus \approx 1$ eV cm^{-2}s^{-1}sr^{-1} is the observed energy flow of EHECR at 100 EeV and $l_E(E_\gamma)$ the photon attenuation length. Additional normalization factors of order unity have not been reproduced here. In other words, for TD or relics to explain the observed EHECR flux at 100 EeV and assuming an X mass of 10^{16} GeV their production or decay rates must be larger than 10^{-46}cm^{-3}s^{-1}. This is of course only an order of magnitude calculation which may be modified by the decay dynamics and the distribution of the X-particles, but can be used as a reasonable benchmark of the necessary rates.

4.3.3. *More about X-particles*

Topological defects

The very wide variety of topological defect models together with their large number of parameters makes them difficult to review in detail. Many authors have addressed this field. Among them let us mention Vilenkin and Shellard[60] and Vachaspati[61,62] for a review on TD formation and interaction, and Bhattacharjee,[63] Bhattacharjee and Sigl[46] and Berezinky, Blasi and Vilenkin[65] for a review on experimental signatures in the framework of the EHECR.

According to the current picture on the evolution of the Universe, several symmetry breaking phase transitions such as $GUT \Longrightarrow H \ldots \Longrightarrow SU(3)\times SU(2)\times U(1)$ occurred during the cooling. For those "spontaneous" symmetry breakings to occur, some scalar field (called the Higgs field) must acquire a non vanishing expectation value in the new vacuum (ground) state. Quanta associated to those fields have energies of the order of the symmetry breaking scale, e.g. $10^{15} - 10^{16}$ GeV for the Grand Unification scale. Such values are indeed perfectly in the range of interest for the above mentioned X-particles.

During the phase transition process, non causal regions may evolve towards different states in such a way that at the different domain borders, the Higgs field keeps a null expectation value. Energy is then trapped in a TD whose properties depend on the topology of the manifold where the Higgs potential reaches its minimum (the vacuum manifold topology).

Possible TDs are classified according to their dimensions: magnetic monopoles (0-dimensional, point-like); cosmic strings (1-dimensional); a sub-variety of the previous which carries current and is supra-conducting; domain walls (2-dimensional); textures (3-dimensional). Among those, only monopoles and cosmic strings are of interest as possible EHECR sources: textures do not trap energy while domain walls, if they existed, would over-close the Universe.[66]

In GUT theories, magnetic monopoles always exist because the reduced symmetry group contains at least the electromagnetic $U(1)$ invariance. In fact it is the predicted over abundance of magnetic monopoles in our present universe that led Guth[67] to come up with the now well adopted idea of an inflationary universe. Strings on the other hand are the only defects that can be relevant for structure formation. It is possible, from the scaling property of the string network, to relate the string formation scale η to the mass fluctuations in the Universe. Using the large scale mass fluctuation value of $\delta M/M \sim 1$ this gives $\eta \simeq 10^{16}$ GeV and similar conclusions are drawn if one uses the COBE results on CMB anisotropies.[68] It is striking to see that if strings were to play a role in large scale structure formation, hence making the Hot Dark Matter scenario viable, the energy scale at which this would be possible also corresponds to that relevant for EHECR production.

When two strings intercommute, the energy release sometimes leads to the production of small loops that will release more energy when they collapse. These are, among other mechanisms, fundamental dissipation processes that prevent the string network from dominating the energy density in the Universe. For monopoles, it is the annihilation of monopolonia (monopole-antimonopole bound states)[69,70] that releases energy.[g] In each case part of the released energy is in the form of X-particles.

Strings and monopoles come in various forms according to the scale at which TDs are formed and to the vacuum topology. They may even coexist. Nevertheless, the X-particle production rate may, on dimensional grounds, be parametrized in a very general way.[71] Introducing the Hubble time t, the production rate can be written as:

$$\dot{n}_X(t) = \frac{Q_0}{m_X}\left(\frac{t}{t_0}\right)^{-4+p} \tag{9}$$

where $Q_0 \equiv \dot{n}_X(t_0)\, m_X$ is the energy injection rate at $t = t_0$ (the present epoch). The parameter p depends on the exact TD model. In most cases (intercommuting strings, collapsing loops as well as monopolonium annihilation) $p = 1$ but superconducting string models can have $p \leq 0$ while decaying vortons[h] give $p = 2$.

One can compare the integrated energy release of Eq. (9) in the form of low energy (10 MeV - 100 GeV) photons resulting from the cascading of the electro-

[g] In fact monopolonia are too short lived but monopole-anti-monopole pairs connected by a string have appropriate lifetime. This happens when the $U(1)$ symmetry is further broken into Z_2.
[h] Superconducting string loops stabilized by the angular momentum of the charge carriers.

magnetic component of the X-particle decay into the diffuse extragalactic gamma ray background, $w_{\rm em} \sim 10^{-6}$ eV cm^{-3} s^{-1}, as measured by EGRET. Assuming as in Ref.[65] that half of the energy release goes into the electromagnetic component, one obtains :

$$w_{\rm em} = \frac{Q_0}{2} \int_{t_{\rm min}}^{t_0} \left(\frac{t}{t_0}\right)^{-4+p} \frac{dt}{(1+z)^4}. \tag{10}$$

where $(1+z) = (t_0/t)^{2/3}$ in a matter dominated Universe. For $\alpha \equiv p - 1/3 > 0$ evolutionary effects are negligible and Eq. (10) simply leads to

$$w_{\rm em} \simeq \frac{Q_0}{2} \frac{t_0}{\alpha}$$

or, using the EGRET limit and $t_0 \simeq 2 \times 10^{17} h^{-1}$s, to:

$$\dot{n}_X(t_0) \le \alpha \frac{10^{-48} h \ {\rm cm}^{-3} {\rm s}^{-1}}{m_X/10^{16}\,{\rm GeV}}$$

a limit hardly compatible with the order of magnitude given by Eq. (8). However, more information about the EHECR fluxes, the diffuse gamma ray background and extragalactic magnetic fields are needed to confirm this trend.

In the models where $\alpha < 0$ evolutionary effects can become important. In fact it is the lower bound of the integral of Eq. (10) that would dominate. Using as a lower bound the decoupling time $t_{\rm dec}/t_0 \sim 10^{-5}$ one gets:

$$w_{\rm em} \simeq \frac{Q_0}{2} \left(\frac{t_{\rm dec}}{t_0}\right)^{-\alpha} \frac{t_0}{|\alpha|}$$

or,

$$\dot{n}_X(t_0) \le |\alpha| \frac{10^{-48-5\alpha} {\rm cm}^{-3} {\rm s}^{-1}}{m_X/10^{16}\,{\rm GeV}}.$$

which, for $p \le 0$ is perfectly compatible with Eq. (8). However the large density of gamma rays released in the early Universe impacts on the ^{4}He production and on the uniformity of the CMB making this kind of models currently unfavored in the context of EHECR.

Supermassive relics

Supermassive relic particles may be another possible source of EHECR.[64] Their mass should be larger than 10^{12} GeV and their lifetime of the order of the age of the Universe since these relics must decay now (close by) in order to explain the EHECR flux. Unlike strings and monopoles, but like monopolonia, relics aggregate under the effect of gravity like ordinary matter and act as a (non thermal) cold dark matter component. The distribution of such relics should consequently be biased towards galaxies and galaxy clusters. A high statistics study of the EHECR arrival distributions will be a very powerful tool to distinguish between aggregating and non-aggregating Top-Down sources.

If one neglects the cosmological effects, a reasonable assumption on the decay rate would simply be, since the decay should occur over the last 100 Mpc/c:

$$\dot{n}_X = \frac{n_X}{\tau}$$

where τ is the relic's lifetime and where the relic density n_X may be given in terms of the critical density of the Universe ρ_c as:

$$n_X = \frac{\rho_c(\Omega_X h^2)}{m_X} = 10^{-17}(\Omega_X h^2)\left(\frac{m_X}{10^{12}\ \mathrm{GeV}}\right)^{-1}$$

From which, with the constraint given by Eq. (8) and using $m_X = 10^{12}$ GeV, one obtains a lifetime of the order of $10^{21}(\Omega_X h^2)$ years. To obtain such a value, orders of magnitude larger than the age of the Universe, one needs a symmetry (such as R-parity) to be very weakly broken (wormhole effect, instanton induced decays) unless the fractional abundance Ω_X represents only a tiny part ($\sim 10^{-11}$) of the density of the Universe, in which case the production mechanism of relics must be extraordinarily inefficient.

4.4. *Conclusions*

The cosmic rays' chemical composition, the shape of their energy spectrum and the distribution of their directions of arrival will prove to be powerful tools to distinguish between the different acceleration or decay scenarios.

If the EHECR are conventional hadrons accelerated by Bottom-Up mechanisms, they should point back to their sources, with a quite specific distribution in the sky and a spectrum clearly showing the GZK cutoff. If, on the other hand, the accelerated particles are not conventional, they should in any case be charged particles (otherwise they can only be secondary collision products) weakly interacting with the CMB but strongly with the atmosphere.

For Top-Down mechanisms and above the ZeV, one should observe a flux of photons (and neutrinos) as the photon absorption length increases (up to several Gpc). Below 100 EeV the spectrum shape will depend on the relative values of, the characteristic distance between TD interactions or relic particle decays and Earth (D), the proton attenuation length (R_p), and the photon absorption length (L_γ). Following the description of Ref.[65] the following situations can be disentangled:

- $R_p < D$: a very low flux with an exponential cutoff. If the sources are nearby, the observed distribution will be strongly anisotropic.

- $L_\gamma < D < R_p$: the protons dominate and the GZK cutoff is visible. As energy increases, the direction of arrival distribution should become more and more anisotropic as photons no longer get absorbed.

- $D < L_\gamma$: a very strong flux in the direction of the sources; photons dominate.

- $D \ll L_\gamma$: the GZK cutoff is visible and protons dominate as long as $R_p(E)$ is much larger than $L_\gamma(E)$. Photons dominate above a few ZeV. The arrival distribution is isotropic at all energies.

For relic particles and TDs like vortons and monopolonia, because of the accumulation in the galactic halo, photons will dominate the flux over the extragalactic contribution. Some anisotropy should be visible due to the earth's slightly eccentric position in the halo. The spectrum will not show any GZK cutoff and the EGRET constraints on the injection rate will not apply as the emitted photons have no time to cascade over the short distances.

Finally, if nuclei can possibly be EHECR candidates in Bottom-Up scenarios, they are completely excluded in the Top-Down cascades.

5. Next

The current EHECR studies essentially rely on the AGASA detector, described in section 3.2. Since 1990, the date of its start, it has reported about 40 events with energies above 40 EeV out of which 7 exceed 100 EeV. Well adapted for the exploration of the spectrum between 1 and 50 EeV, its major role for the physics beyond the GZK cutoff is the confirmation that something new is happening there. A systematic exploration of this region hopefully bringing an answer to the question "What and How?" will come from the detectors and projects that we will describe here. To compare the performances of the future detectors or projects, we propose to use, as a reference, the flux rate formula given in Eq. 1.

5.1. *The present: HiRes*

The "High Resolution Fly's Eye" or HiRes[72] is an improved version of the original Fly's Eye detector (section 3.2). The present version of the detector design consists of two "Eyes" separated by 13 km, situated at a military site in Dugway (Utah, USA). The basic fluorescence telescope of HiRes is a mirror equipped with a camera of 256 phototubes, each phototube (pixel) watching an angular region of space of $1° \times 1°$. Therefore, each telescope has a field of view of $16° \times 16°$, and a complete eye is expected to cover a field of 30° in elevation and 360° in azimuth with 44 telescopes. The collaboration expects to have one full and one half eyes by the end of 1999. The fluorescence light emitted by the EAS can be seen by such telescopes at distances up to 20 km or more depending on their energy. The aperture of the detector has to be convoluted with its duty-cycle (10%), and is energy-dependent (far showers can be reconstructed only if they are in the higher energy range). Once fully equipped its aperture should be of 350 km^2 sr at 10 EeV and about 1000 km^2 sr at 100 EeV. This gives a detection rate (based on the empirical formula, see above) of about 10 events/year above 100 EeV. The HiRes detector's optimal operating range is therefore the decade between 5 and 50 EeV.

It is interesting to note that the HiRes prototype is overlooking the Chicago AirShower Array (CASA) also installed at Dugway, thus allowing the detection of a few events in the "hybrid" mode.

5.2. *Starting: Auger Observatory*

The Auger Observatory[i] is the only existing or projected detector whose design is based on the "hybrid" detection mode (EAS simultaneously observed by a ground array and a fluorescence detector).[37]

The Observatory whose construction starts during the fall of 1999, once completed, will be covering two sites, respectively in the southern (Pampa Amarilla, province of Mendoza, Argentina) and northern (Millard County, Utah, USA) hemispheres. The southern hemisphere detector is especially interesting since very few detectors took data in the past in this part of the world from where the direction of the center of our galaxy is visible.

The size of the ground array is adapted to its physics aims: explore the spectrum around and above the GZK cutoff. Therefore the surface of each site was chosen to be of 3000 km^2, so as to provide a statistics of a few tens of expected events per year above 100 EeV. The detector is designed to be fully efficient for showers with energies of 10 EeV and above, with a duty-cycle of 100%. This will make the link with the part of the energy spectrum well explored by presently operating or upcoming detectors, AGASA and HiRes. The energy threshold defines the spacing of the detector "stations": with a spacing of 1.5 km between the stations, a 10 EeV vertical shower will hit on average 6 stations which is enough to fully reconstruct the EAS. With such a spacing on a regular grid, the total number of stations is about 1600. Each station is a cylindrical tank (the same basic design as the Haverah Park array, but with much more sophisticated electronics), of 10 m^2 surface and 1.2 m height. The tanks are filled with filtered water in which the secondary particles from the EAS produce light by Cerenkov radiation. The light is reflected and diffused by an internal coating and detected by three phototubes installed on the top. Flash-ADCs cycling at a rate of 40 MHz record the pulse heights as a function of time. With such a system, the separation of the muons from the electromagnetic component of the shower becomes reasonably good.

Because of the size of the array, the stations have to work in a stand-alone mode: they are powered by solar panels and batteries, and the communication with the central station where the data-taking system is installed is done by telecommunication techniques.

The giant array is completed by an optical device detecting the fluorescence light emitted by the nitrogen molecules of the atmosphere excited by the charged particles produced in the EAS. The fluorescence telescopes use pixels (phototubes) with a field of view of 1.5°. A telescope is a camera with 400 pixels installed at the focal plane of a mirror whose size is 3.5×3.5 m^2. Each telescope sees an angle of about 30×30 degrees. On the southern site, three eyes (7 telescopes each) will be installed at the periphery of the array and one (12 telescopes) in the middle, in order for the whole array to be visible by at least one of the telescopes. On

[i] Named after the french physicist Pierre Auger, see Section 3.

the northern site, the optical component *could* be the HiRes we described in the previous section or the Telescope Array which we present in the next one.

In the hybrid mode (10% of the events), the detector is expected to have on average 10% energy resolution and an angular precision of about $0.3°$. For the array alone those numbers become 20% and less than $1°$.

The statistics attainable with such a detector is dependent on what exactly will happen above the GZK cutoff. However, with its total aperture of 14000 km^{2}sr (both sites), the Auger Observatory should detect of the order of 6000 events above 10 EeV and 60 above 100 EeV per year.

5.3. *The future: the Telescope Array*

The Telescope Array[73] (TA) is a project of a purely optical detector which, in its initial design, aims to be used as a gamma-astronomy device as well as a fluorescence detector. Its basic principles are identical to the HiRes technique. The individual telescopes are made of 3 meter diameter segmented mirrors with a camera of 256 pixels. Each pixel (hexagonal phototubes) sees a patch of sky in a solid angle of $1° \times 1°$ (hence a field-of-view of $16° \times 16°$ per telescope). One TA station is made of 42 telescopes, thus viewing the sky over 2π in azimuth and $30°$ in elevation. If the project is approved and completed, the TA collaboration intends to install on the Utah site 8 stations in a snake-shaped pattern which would extend from the present position of the HiRes detector in Dugway to the future northern site of the Auger Observatory in Millard County (about 100 km south of Dugway). Two of the stations would then become the optical component of the Auger array to detect showers in the hybrid mode. The total aperture of the array should be about 5 times the HiRes acceptance, depending on the spacing of the stations and the performance of the pixels.

5.4. *The far future: Airwatch/OWL*

One cannot exclude the possibility that the EHECR spectrum extends to even higher energies than those for which the three above projects were designed. Such a hypothesis would become likely if the production mechanism is one of the top-down models, in which case the spectrum could go well above 1 ZeV. At the same time, the fluxes at these energies would be still smaller than those detectable by Auger. Is there any means of observing with reasonable statistics events in this energy range?

It is easy to see that the ground array method can hardly be envisaged if one, or more, order of magnitude increase in aperture is needed. The aperture is proportional to the surface of the array, and for practical (and to some extent, economical) reasons the present surface of the Auger arrays is close to what can be considered as an upper limit. As for the fluorescence technique, there are two ways of increasing the aperture: increase the number of telescopes and/or increase the sensitivity of the pixels, i.e. the visible depth of field. The former solution is the one envisaged by the Telescope Array collaboration. Here again the cost increases linearly with the aperture. The latter solution is the basic idea of the Airwatch/OWL projects.

The physics aims of both projects is the same as that of the detectors outlined in the preceding sections: solve the puzzle of the origin of the highest energy cosmic rays. The technical solution proposed is similar to that of the Fly's Eye: observe the air-shower's fluorescence light, but from *above* (i.e. by a detector installed in a dedicated or general-purpose satellite) and from a distance of 500 km instead of the 20 km field of view for the ground-based version.

The idea of observing the EAS from space originated from converging ideas of J.Linslay at the end of the seventies and a proposal made by Y.Takahashi during the mid-nineties for a Maximum-energy Air Shower observing Satellite (MASS). The project was then promoted in parallel in Europe (mainly Italy) under the name of Airwatch,[74] and in the USA (with the support of NASA and participation of Japanese groups) in its OWL[75] (Orbiting Wide-angle Light collectors) version. The basic idea is to use about 10^6 highly sensitive pixels at the focal plane of a wide angle (30° cone) optical system (Fresnel lenses and reflectors). Several options are being studied for the pixels. The expected performances would be: a resolution of 1 km from a distance of 500 km, 1 photoelectron sensitivity of the pixels, very good background rejection (city lights, atmospheric phenomena) and, finally, an effective aperture of 10^5 km^{2}sr, increasing that of the Auger Observatory by a factor of 10. A good reconstruction of the showers, as with the ground based fluorescence detectors, needs a stereo view, therefore two satellites. The project still needs a large R&D effort. Adding to it the funding and construction of the detector, it is reasonable to assume that the it will not be operational before ten years or so.

6. Conclusions

The EHECR were a puzzle when they were first observed, more than 30 years ago. They still are. In our review we tried to show that this statement is true to a large extent. This does not mean that theorists find no explanation as to their existence, but rather that their models are either not fully convincing (in the sense that they do not explain the full set of observed data in the field) or based on exotic, and as such still-to-be-confirmed, theories.

The past experiments which explored this field could do hardly better than convince us of the existence of the EHECR above the GZK cutoff. Statistics which should make us able to locate the sources, reconstruct the shape of the CR spectrum above the cutoff and study the CR chemical composition will soon be provided by the ongoing (HiRes, AGASA) and oncoming (Auger, Telescope-Array, OWL/Airwatch) experiments.

We shall leave the last (but hopefully provisional) word to L.Celnikier[76] who, in a review article written a few years ago, concluded: "Contemporary astrophysics is faced by a number of acute problems. One of them concerns dark matter, which one might (perhaps mischievously) qualify as the study of particles which *should* exist ... but until farther notice, don't. Ultra high energy cosmic rays constitute the inverse problem: particles which *do* exist ... but perhaps shouldn't." To our best knowledge, the statement is still actual both ways.

Acknowledgements

The authors have made, for this article, extensive use of the work produced over the past three years in the framework of the Pierre Auger project. We are grateful to many of the members of this collaboration and, indeed, specifically to the project spokespersons James W.Cronin and Alan A.Watson for their availability for so many stimulating discussions. Also many thanks to P.Billoir and P.Sommers for their useful and perceptive comments, to P.Astier and E.Berman for their careful reading of the manuscript.

References

The references given as astro-ph/xxxxxxx or hep-ph/xxxxxxx are articles available from the Web electronic preprint archive at the URL
`http://xxx.lanl.gov/`

1. K. Greisen, *Phys. Rev. Lett.* **16** (1966) 748.
   G.T.Zatsepin, V.A.Kuzmin, *JETP Lett.* **4** (1966) 78.
2. L. Landau, I. Pomeranchuk, *Dokl. Akad. Nauk. SSR* **92** (1953) 535.
   A. B. Migdal, *Phys. Rev.* **103** (1956) 1811.
3. S. J. Sciutto, "Air Shower Simulations with the AIRES System", astro-ph/9905185.
4. J. N. Capdevielle *et al*, Kernforschungszentrum Karlsruhe preprint KfK 4998 (1992).
   J. Knapp, D. Heck, preprint KfK 5196 (1993).
5. Web site: `osf1.lngs.infn.it/~carboni/Hemas/doc/`
6. A. M. Hillas, *Proc. 19th ICRC (La Jolla)*, **1** (1985) 155.
7. R. Engel, *Xth Int. Symposium on Very High Energy Cosmic Rays Interactions*, Gran Sasso (1998).
8. H. O. Klages *et al* (KASCADE Collaboration), *Nucl. Phys. B (Proc. Suppl.)* **52B** (1997) 92.
9. R. S. Fletcher et al., *Phys. Rev.* **D50** (1994) 5710.
10. K. Werner, *Phys. Rep.* **232** (1993) 87.
11. N. N. Kalmykov, S. S. Ostapchenko, *Yad. Fiz.* **56** (1993) 105.
12. J. Ranft, INFN/AE-97/45, Gran Sasso report, 1997.
13. H. Fesefeldt, Report PITHA-85/02 (1985), RWTH Aachen.
14. J. Knapp, *Proc. 25th ICRC*, Durban (1997).
    T. Antoni *et al*, "Test of high-energy interaction models using the hadronic core of EAS", astro-ph/9904287.
15. A. D. Erlykin, A. W. Wolfendale, *Astropart. Phys.* **9** (1998) 213.
16. K. Greisen, *Ann. Rev. Nucl. Sc.* **10** (1960) 63.
    K. Suga, *Proc. 5th Interamerican Seminar on Cosmic Rays*, La Paz (Bolivia) 1962.
17. G. L. Cassiday, *Ann. Rev. Nucl. Part. Sci.* **35** (1985) 321. See also Ref.[19], Chapter 6.
18. A. M. Hillas, *J. Phys. G: Nucl. Phys.* **8** (1982) 1461.
19. For a clear and detailed presentation of EAS properties, see e.g. P. Sokolsky, *Introduction to Ultra High Energy Cosmic Ray Physics* (Addison Wesley, Frontiers in Physics, 1989), Chapter 3.
20. M. A. Lawrence, R. J. O. Reid, A. A. Watson, *J. Phys. G.* **17** (1991) 773.

21. S. Yoshida *et al*, *Astropart. Phys.* **3** (1995) 105.
22. R. Gandhi *et al*, *Astropart. Phys.* **5** (1996) 81.
23. K. S. Capelle, J. W. Cronin, G. Parente, E. Zas, *Astropart. Phys.* **8** (1998) 321.
    P. Billoir, "Neutrino capabilities of the AUGER detector", *8th International Workshop on Neutrino Telescopes*, Venice, 1999.
    S. Coutu, X. Bertou, P. Billoir, "Ultra-high energy neutrinos with Auger", *John Hopkins Workshop (Neutrinos in the Next Millenium)*, 1999 (submitted to World Scientific).
24. P. Auger, R. Maze, T. Grivet-Meyer, *Comptes rendus, Académie des Sciences* **206** (1938) 1721.
    P. Auger, R. Maze, *Comptes rendus, Académie des Sciences* **207** (1938) 228.
    P. Auger *et al*, *Rev. Mod. Phys.* **11** (1939) 288.
25. S. Swordy, private communication. The data points are collected from the following experiments: LEAP, Proton, Akeno, AGASA, Fly's Eye, Haverah Park, Yakutsk.
26. A. A. Watson, Proc. of the 1998 Nobel Symposium, Stockholm, August 1998 (to be published).
27. J. Linsley, *Phys. Rev. Lett.* **10** (1963) 146.
28. D. J. Bird *et al*, *Ap. J.* **424** (1994) 491.
29. B. N. Afanasiev *et al*, *Proc. of the 24th ICRC*, Rome, Italy **2** (1995) 756.
30. For a complete and comprehensive overview of the astrophysical acceleration mechanisms, see M. S. Longair, in *High Energy Astrophysics* (Cambridge University Press, Cambridge, 2nd edition, 1994), Vol. 2, Chapter 21 and T. K. Gaisser, *Cosmic Rays and Particle Physics* (Cambridge University Press, Cambridge, 1990), Chapter 11.
31. M. Takeda *et al*, *Phys. Rev. Lett.* **81** (1998) 1163; e-print astro-ph/9807193.
    See also: `www.icrr.u-tokyo.ac.jp/as/project/agasa.html`, the AGASA Web site for regular updates.
32. N. Hayashida *et al*, *J. Phys. G.* **21** (1995) 1101. For recent updates, see also: `www.icrr.u-tokyo.ac.jp/as/project/agasa.html`.
33. B. R. Dawson, R. Meyhandan, K. M. Simpson, *Astropart. Phys.* **9** (1998) 331.
34. F. Halzen *et al*, *Astropart. Phys.* **2** (1995) 151.
35. P. P. Kronberg, *Rep. Prog. Phys.* **57** (1994) 325.
36. J. P. Vallée, *Ap. J.* **366** (1991) 450.
37. *The Pierre Auger Project Design Report*, Fermilab, October 1995 (Web site: `www.auger.org/admin/`).
38. M. Lemoine, G. Sigl, P. Biermann, "Supercluster Magnetic Fields and Anisotropy of Cosmic Rays above 10^{19} eV", astro-ph/9903124.
39. G. R. Farrar, T. Piran, "GZK Violation - a Tempest in a (Magnetic) Teapot?", astro-ph/9906431.
40. M. Takeda *et al*, "Small scale anisotropy of cosmic rays above 10^{19} eV observed with the Akeno Giant Air Shower Array", astro-ph/9902239.
41. N. Hayashida *et al*, "The anisotropy of cosmic ray arrival directions around 10^{18} eV", astro-ph/9807045, *Astropart. Phys.* **10** (1999) 303.
42. D. J. Bird *et al*, "Study of Broad Scale Anisotropy of Cosmic Ray Arrival Directions from 2×10^{17} eV to 10^{20} eV from Fly's Eye data", astro-ph/9806096.
43. C. Cesarsky, Proc. of the International Workshop on Techniques to Study Cosmic Rays with Energies Greater than 10^{19} eV, Paris, *Nucl. Phys. B (Proc. Suppl.)* **28B** (1992) 51.
    C. Cesarsky, V. Ptuskin, Proc. 23rd ICRC (Calgary), **2** (1993) 341.
44. J. W. Cronin, private communication, unpublished.
45. R. D. Blanford, "Acceleration of ultra high energy cosmic rays", e-print astro-ph/9906026 (to be published in *Particle Physics and the Universe, Physica Scripta*

World Scientific.).
46. P. Bhattacharjee, G. Sigl, "Origin and propagation of extremely high energy cosmic rays", astro-ph/9811011, to be published in Physics Reports.
47. I. F. M. Albuquerque, G. R. Farrar, E. W. Kolb, *Phys.Rev.* **D59** (1999).
48. A. Karle *et al*, *Phys. Rev. Lett.* **B347** (1995) 161.
49. G. Sigl, M. Lemoine, P. Biermann, *Astropart. Phys.* **10** (1999) 141.
50. A. Venkatesan, M. Coleman Miller, A. V. Olinto, *Ap. J.* **484** (1997) 323.
51. F. Halzen, E. Zas, *Ap. J.* **488** (1997) 669.
52. R. J. Protheroe "Origin and propagation of the highest energy cosmic rays", Towards the Millennium in Astrophysics: Problems and Prospects, Erice 1996, eds. M.M. Shapiro and J.P. Wefel (World Scientific, Singapore).
53. L. O'C. Drury, *Rep. Prog. Phys.* **46** (1983) 973.
54. J. G. Kirk and P. Duffy, "Particle acceleration and relativistic shocks", astro-ph/9905069.
55. A. M. Hillas, *Annual Review Astron. Astrophys.* **22** (1984) 425.
56. P. L. Biermann, *Phys. Rev.* **D51** (1995) 3450.
57. G. R. Farrar, P. L. Biermann, *Phys. Rev. Lett.* **81** (1998) 3579.
58. B. Andersson et al. *Phys. Rep.* **97** (1983) 31.
59. Y. I. Azimov et al. *Z. Phys. C* **27** (1985) 65.
60. A. Vilenkin, E. P. S. Shellard, "Strings and Other Topological Defects", Cambridge Univ. Press, Cambridge, 1994.
61. T. Vachaspati, "Formation of Topological Defetcs", ICTP summer school on Cosmology (1997), hep-ph/9710292.
62. T. Vachaspati, "Formation, Interaction and Observation of Topological Defects", Les Houches (1998), astro-ph/9903362.
63. P. Bhattacharjee, "Ultrahigh Energy Cosmic Rays from Topological Defects — Cosmic Strings, Monopoles, Necklaces, and All That", astro-ph/9803029.
64. V. Berezinsky, *"Ultra High Energy Cosmic Rays"*, hep-ph/9802351
65. V. Berezinsky, P. Blasi, A. Vilenkin, *Phys. Rev.* **D58** (1998), 103515.
66. Ya. B. Zel'dovich, I. Kobzarev, L. Okun, *Zh. Eksp. Teor. Fiz.* **67** (1974) 3.
67. A. H. Guth, *Phys. Rev.* **D23** (1981) 347.
68. R. H. Brandenberger, *Pramana* **51** (1998) 191. See also hep-ph/9806473.
69. C. T. Hill, *Nucl. Phys.* **B 224** (1983) 469.
70. D. N. Schramm, C. T. Hill, Proc. 18th ICRC (1983) 393.
71. P. Bhattacharjee, C. T. Hill, D. N. Schramm, *Phys. Rev. Lett.* **69** (1992) 567.
72. S. C. Corbato *et al*, Proc. of the International Workshop on Techniques to Study Cosmic Rays with Energies Greater than 10^{19} eV, Paris, *Nucl. Phys. B (Proc. Suppl.)* **28B** (1992) 36.
    Web site: `sunshine.chpc.utah.edu/research/cosmic/hires/`
73. Web site: `www-ta.icrr.u-tokyo.ac.jp/`
74. Web site: `www.ifcai.pa.cnr.it/~AirWatch/AWhome.html`
    O.Catalano *et al*, Proc. of the 19th TEXAS Symposium on Relativistic Astrophysics, 1998.
75. Web site: `owl.gsfc.nasa.gov/`
76. L. K. Celnikier, "Desperately seeking the source of ultra high energy cosmic rays", *Proc. Rencontres de Moriond, February 1996* (Editions Frontières).